

1 Phytoplankton composition from sPACE: requirements,  
2 opportunities, and challenges

3 Ivona Cetinić <sup>a,b,1</sup>, Cecile S. Rousseaux <sup>b,\*,1</sup>, Ian T. Carroll <sup>c,b</sup>, Alison P. Chase <sup>d</sup>, Sasha J. Kramer <sup>e</sup>, P. Jeremy  
4 Werdell <sup>b</sup>, David. A. Siegel <sup>f</sup>, Heidi M. Dierssen <sup>g</sup>, Dylan Catlett <sup>h</sup>, Aimee Neeley <sup>b,i</sup>, Inia M. Soto Ramos <sup>a,b</sup>,  
5 Jennifer L. Wolny <sup>j</sup>, Natasha Sadoff <sup>b,i</sup>, Erin Urquhart <sup>b,i</sup>, Toby K. Westberry <sup>k</sup>, Dariusz Stramski <sup>l</sup>, Nima  
6 Pahlevan <sup>m,i</sup>, Bridget N. Seegers<sup>a,b</sup>, Emerson Sirk <sup>b,i</sup>, Priscila Kienteca Lange <sup>n,o</sup>, Ryan A. Vandermeulen <sup>b,l,#</sup>,  
7 Jason R. Graff<sup>k</sup>, James G. Allen<sup>p</sup>, Peter Gaube<sup>d</sup>, Lachlan I. W. McKinna<sup>q</sup>, S.Morgaine McKibben<sup>r</sup>, Caren E.  
8 Binding<sup>s</sup>, Violeta Sanjuan Calzado<sup>c,b</sup>, Michael Sayers<sup>t</sup>

9 <sup>a</sup>GESTAR II, Morgan State University, Baltimore, Maryland, USA

10 <sup>b</sup>Ocean Ecology Laboratory, NASA Goddard Space Flight Center, Greenbelt, Maryland, USA

11 <sup>c</sup>GESTAR II - University of Maryland Baltimore County, Baltimore, Maryland, USA

12 <sup>d</sup>Applied Physics Laboratory, University of Washington, Seattle, Washington, USA

13 <sup>e</sup> Monterey Bay Aquarium Research Institute, Moss Landing, California, USA

14 <sup>f</sup> Earth Research Institute, University of California, Santa Barbara, Santa Barbara, California, USA

15 <sup>g</sup>Department of Marine Sciences, University of Connecticut, Groton, Connecticut, USA

16 <sup>h</sup>Biology Department, Woods Hole Oceanographic Institution, Woods Hole, Massachusetts, USA

17 <sup>i</sup> Science Systems and Applications, Inc., Greenbelt, Maryland, USA

18 <sup>j</sup> Office of Regulatory Science, Center for Food Safety and Applied Nutrition, US Food and Drug  
19 Administration, College Park, Maryland, USA

20 <sup>k</sup> Department of Botany and Plant Pathology, 2071 SW Campus Way, Oregon State University, Corvallis,  
21 OR, USA

22 <sup>l</sup> Marine Physical Laboratory, Scripps Institution of Oceanography, University of California San Diego, La  
23 Jolla, California 92093-0238, USA

24 <sup>m</sup> Terrestrial Information Systems Laboratory, NASA Goddard Space Flight Center, Greenbelt, Maryland,  
25 USA

26 <sup>n</sup> Departamento de Meteorologia, Universidade Federal do Rio de Janeiro, Rio de Janeiro, Brazil

27 <sup>o</sup> Blue Marble Space Institute of Science, Seattle, USA

28 <sup>p</sup> Department of Oceanography, School of Ocean and Earth Science and Technology, University of Hawai'i  
29 at Mānoa, Honolulu, Hawai'i, USA

30 <sup>q</sup> 3Go2Q Pty Ltd., Sunshine Coast, Queensland, Australia

31 <sup>r</sup> NASA Postdoctoral Program/NASA Goddard Space Flight Center, Greenbelt, Maryland, USA

32 <sup>s</sup> Water Science and Technology Directorate, Environment and Climate Change Canada, Burlington,  
33 Ontario, Canada

34 <sup>t</sup> Michigan Tech Research Institute, Michigan Technological University. Ann Arbor, Michigan, USA

35 <sup>#</sup>Present address: National Marine Fisheries Service, National Oceanic and Atmospheric Administration,  
36 Silver Spring, MD, USA

37 \* Corresponding author

38 <sup>1</sup> Ivona Cetinić and Cecile S. Rousseaux contributed equally

39

## 40 Abstract

41 Ocean color satellites have provided a synoptic view of global phytoplankton for over 25 years  
42 through surface measurements of the concentration of chlorophyll a. While remote sensing of  
43 ocean color has revolutionized our understanding of phytoplankton and their role in the oceanic  
44 and freshwater ecosystems, it is important to consider both total phytoplankton biomass and  
45 changes in phytoplankton community composition in order to fully understand the dynamics of  
46 the aquatic ecosystems. With the upcoming launch of NASA's Plankton, Aerosol, Clouds, ocean

47 Ecosystem (PACE) mission, we will be entering into a new era of global hyperspectral data, and  
48 with it, increased capabilities to monitor phytoplankton diversity from space. In this paper, we  
49 analyze the needs of the user community, review existing approaches for detecting  
50 phytoplankton community composition in situ and from space, and highlight the benefits that  
51 the PACE mission will bring. Using this three-pronged approach, we highlight the challenges and  
52 gaps to be addressed by the community going forward, while offering a vision of what global  
53 phytoplankton community composition will look like through the “eyes” of PACE.

## 54 1. Background

55 Phytoplankton are microscopic, photosynthetic organisms that inhabit all sunlit waters and  
56 represent the first level of the aquatic food web. They play a vital role in the global ecosystem  
57 where phytoplankton convert carbon dioxide into carbohydrates and oxygen through the process  
58 of photosynthesis. The primary photosynthetic pigment in most phytoplankton species is  
59 Chlorophyll a (*Chl a*), which has been commonly used as a proxy for phytoplankton biomass in  
60 oceanographic research and monitoring programs for almost 100 years (Harvey 1934). Global  
61 ocean color satellites (SeaWiFS, MODIS, VIIRS) have provided continuous global datasets of  
62 aquatic *Chl a* since 1997 (O’Reilly et al. 1998), generating insight into spatial and temporal changes  
63 in phytoplankton biomass (Behrenfeld et al. 2006; Gregg and Rousseaux 2014; Gregg et al. 2017;  
64 McClain et al. 2022; Siegel et al. 2013). Despite the ubiquity of *Chl a*, taxonomic diversity in  
65 phytoplankton is wide-ranging, spanning across eukaryotic and eubacterial domains. This  
66 taxonomic diversity underpins vast morphological diversity among phytoplankton (e.g., Beardall  
67 et al. 2009), including variation in pigment composition (e.g., Jeffrey et al. 2011), environmental  
68 requirements (e.g., for light, nutrients, and temperature), trophic strategies (e.g., Mitra et al.

69 2016), and in the roles phytoplankton play in aquatic biogeochemistry (e.g., Dutkiewicz et al.  
70 2020).

71 Knowledge of phytoplankton community composition (PCC) and its spatial and temporal  
72 variability is vital for our understanding of the many aspects of aquatic ecosystems, as well as the  
73 services those ecosystems provide. It is critical to assess water quality (including harmful algal  
74 blooms - HABs) and functioning of the higher trophic levels including fisheries worldwide.  
75 Knowledge about PCC can be used to manage and support the aquaculture industry, including to  
76 infer optimal site selection and sustainable aquaculture development<sup>1</sup> (Anderson et al. 2009;  
77 2019; Johnson et al. 2019; Snyder et al. 2017), to prevent economic losses due to the impact of  
78 HABs (Smith and Bernard 2020; Wolny et al. 2020), or to support monitoring of potential impacts  
79 that aquaculture might have on aquatic ecosystems (e.g., eutrophication; Gowen 1994) or on  
80 natural phytoplankton population estimates (Schaeffer et al. 2015; Frieder et al. 2022).  
81 Additionally, PCC can enhance the parameterization of end-to-end ecosystem models designed  
82 to simulate biogeochemical, ecological, fishery, management, and socio-economic processes  
83 within marine ecosystems (Turner et al. 2021; Caracappa et al. 2022).

84 Furthermore, to understand the effects of climate variability on aquatic biogeochemistry, the role  
85 of the oceans as a sink of anthropogenic carbon, and the various effects of human pressure on  
86 water resources, it is imperative that we improve our characterization of the food web's  
87 foundation—the phytoplankton community—across the continuum of aquatic ecosystems.  
88 Understanding the role that different phytoplankton groups play in the export of carbon,

---

<sup>1</sup> ShellGIS, an application developed to predict growth of numerous aquaculture species using remote sensing inputs, <http://www.shellgis.com/examples/TFWMidMaine.html>. ShellGIS team is part of the PACE early adopter program.

89 specifically in regard to ballasting, export depths and scales of remineralization (Cram et al. 2018;  
90 Guidi et al. 2015), is crucial to our understanding of contemporary and future oceans. Currently,  
91 there is also much debate as to the future of the ocean's role in absorbing anthropogenic carbon,  
92 as well as the role that biology, specifically different phytoplankton types, will play in different  
93 climate scenarios. Earth System Models (ESMs) are used to understand and forecast the role of  
94 oceans in the global carbon budget, including the role of oceans in future climate scenarios (IPCC<sup>2</sup>,  
95 CMIP<sup>3</sup>, etc). For most ESMs, understanding the role that biology will have in future carbon  
96 sequestration relies on our understanding of oceanic PCC, in part due to the relationship between  
97 phytoplankton size and sinking rate (i.e., Guidi et al. 2015; Henson et al. 2022).

98 Whether categorized by taxa, function, or size, the particular mix of phytoplankton detectable by  
99 in situ sampling is discernably variable across regions, seasons, and conditions; underscoring a  
100 strong need for studying what we collectively call PCC through ocean remote sensing. During the  
101 past 25 years, numerous studies have shown that space-based instruments can reach beyond  
102 estimates of total phytoplankton biomass and quantify certain aspects of PCC (e.g., Bracher et al.  
103 2017; IOCCG 2014). Such insights on PCC have mostly relied on *Chl a* or multi-band phytoplankton  
104 absorption spectra (see Mouw et al. 2017 and references within), information that inherently  
105 creates large uncertainties from the inverse problem standpoint, i.e., solving for various  
106 components of PCC from a limited number of observations (Defoin-Platel and Chami 2007; Sydor  
107 et al. 2004).

---

<sup>2</sup> IPCC stands for Intergovernmental Panel on Climate Change, <https://www.ipcc.ch/>

<sup>3</sup> CMIP stands for World Climate Research Programme Coupled Model Intercomparison Project, <https://www.wcrp-climate.org/wgcm-cmip>

108 As the needs of aquatic research surpassed the capabilities of current ocean color satellites, the  
109 community responded with various instrument concepts, materialized in specific calls by the  
110 National Research Council Earth Sciences Decadal Survey (National Research Council 2007) and  
111 National Aeronautics and Space Administration (NASA, NASA 2010) among others (McClain et al.  
112 2022; Muller-Karger et al. 2018). The need to resolve taxonomic components of PCC is one of the  
113 main underlying motivations for NASA's Plankton, Aerosol, Cloud, ocean Ecology (PACE) mission  
114 (Werdell et al. 2019). The PACE mission, to be launched no earlier than January 2024, will respond  
115 to community needs for a highly calibrated, ocean-focused hyperspectral radiometer combined  
116 with multi-angle polarimeters that satisfy multiple scientific needs, including better resolution of  
117 phytoplankton diversity (McClain et al. 2022; Werdell et al. 2019).

118 PACE is the first global ocean and atmosphere hyperspectral mission (Figure 1). PACE will collect  
119 ocean color imagery over a period of one-to-two days from a sun-synchronous polar orbit at 676.5  
120 km (inclination of 98°), with an ascending equatorial crossing time at 1 pm. The spacecraft will  
121 host three instruments: a hyperspectral imaging radiometer named OCI (for Ocean Color  
122 Instrument, developed by NASA Goddard Space Flight Center (GSFC)) and two polarimeters,  
123 named SPEXone (for Spectro-polarimeter for Planetary Exploration, developed by collaborators  
124 at Space Research Organization of the Netherlands, Hasekamp et al. 2019) and HARP2 (for Hyper  
125 Angular Research Polarimeter, developed by the Earth and Space Institute of the University of  
126 Maryland Baltimore County, Martins et al. 2002).

127 The OCI has hyperspectral capabilities that continuously span from the ultraviolet to near-  
128 infrared, with nominal spectral steps of 2.5 nm and average bandwidths of ~5 nm across a  
129 spectral range of 340-890 nm. The spectral steps decrease to 1.25 nm (with the same ~5 nm

130 bandwidths) in the spectral regions of chlorophyll a fluorescence and oxygen A and B band  
131 absorption, resulting in roughly 230 total wavelengths of information (Table 1). Additional bands  
132 in the near- and shortwave-infrared support heritage atmospheric products and will also bring  
133 improvements to atmospheric correction in optically complex waters over large freshwater and  
134 coastal estuaries (Frouin et al. 2019; Ibrahim et al. 2018). The spatial resolution of OCI imagery  
135 will be  $\sim 1 \text{ km}^2$  at nadir with a swath width of 2663 km (supporting global coverage once every  
136 two days, given geometry constraints applied to atmospheric correction). In practice, pixels sizes  
137 at the center of the swath will be  $\sim 1.1 \text{ km}^2$  given OCI's 20-deg tilt. Due to the specific optical  
138 design, time-delayed integration, lunar, spectral calibrations, and tilt mechanism OCI will produce  
139 high-quality data over a very high dynamic range of radiances from highly absorbing waters to  
140 ecosystems rich in inorganics.

141 The role of the two PACE polarimeters, SPEXone and HARP2 (Table 1), is primarily to improve our  
142 understanding of cloud and atmospheric aerosol properties (Chowdhary et al. 2019; Remer et al.  
143 2019; Sayer et al. 2022). Improved characterization of the atmospheric properties will enhance  
144 the retrieval of ocean surface reflectances, and there is hope that information about the  
145 microphysical properties of particles from polarimeters may also prove useful for phytoplankton  
146 studies (Jamet et al. 2019). SPEXOne is a hyperspectral polarimeter (385-770 nm, 5 nm steps),  
147 measuring light at 5 viewing angles, collecting information in narrow 100 km swath at  $2.5 \text{ km}^2$ .  
148 HARP2 is a multispectral (nominal 441, 549, 665, 866 nm), hyper-angular instrument, with a wide  
149 swath that matches OCI and a ground sampling distance of  $3 \text{ km}^2$ .

150 By identifying the needs, challenges, and future of estimating PCC from space using hyperspectral  
151 instruments, this paper contributes to a decades-long community effort to improve remotely-

152 sensed phytoplankton datasets (e.g., Bracher et al. 2017; Bracher et al. 2022; IOCCG 2014; Mouw  
153 et al. 2017). After evaluating user community needs (Section 2) and identifying several  
154 applications that will benefit from improved PCC estimates (Section 3), we outline current  
155 approaches to identifying PCC using in situ data, a critical step in developing PCC retrieval  
156 algorithms (Section 4). We then describe the existing approaches that PACE will build on to derive  
157 PCC from space (Section 5). Finally, we conclude the paper by identifying some of the existing  
158 challenges and gaps, address what PCC will mean in the era of PACE, and discuss how PACE will  
159 allow the community to advance understanding of the role that phytoplankton diversity plays on  
160 earth and how it is likely to change in the future.

## 161 2. Community Needs

162 There is a consensus across the ocean color user community that better resolution of  
163 phytoplankton diversity from space will improve our knowledge and understanding of marine  
164 ecosystems (e.g., Kavanaugh et al. 2021), ocean health (e.g., Smith and Bernard 2020), shifts in  
165 communities across freshwaters (Rasconi et al. 2015; Verbeek et al. 2018), and the ocean's effects  
166 on the global climate (IPCC 2019). However, the needed resolution (taxonomic or otherwise) of  
167 phytoplankton diversity varies widely within the user community.

168 A request for input was directed to the PACE Community of Practice<sup>4</sup> (CoP) to identify PCC  
169 taxonomic resolution needs. The PACE CoP is a diverse group of users composed of modelers and  
170 empirical researchers, academic and government scientists, local to international decision-

---

<sup>4</sup> [https://pace.oceansciences.org/app\\_community.htm](https://pace.oceansciences.org/app_community.htm)

171 makers, and industry professionals within various sectors, including air quality and atmospheric,  
172 terrestrial, and marine/ocean applications (Figure 2).

173 Responses indicate that data consumers most need resolution down to a few traditionally  
174 recognized “taxonomic groups” (e.g., diatoms, dinoflagellates), followed by plankton pigments,  
175 and then groups defined by functionality (Figure 3). A large portion of questionnaire respondents  
176 would be satisfied with “whatever taxonomic grouping is available” beyond *Chl a* alone.  
177 Approximately 25% of the users prioritized species-level resolution, with 10% of users relying on  
178 PACE to resolve specific species (such as the HAB forming dinoflagellate *Alexandrium*). While this  
179 short questionnaire provides preliminary insights into the needs of the PACE user community, it  
180 does not provide information on how these needs relate to each subcommunity.

181 The above-mentioned needs are likely driven by the spatiotemporal constraints of each  
182 respondent’s focus, ranging from local to global spatial scales, and from daily, monthly,  
183 interannual, and decadal scales. In a similar way, user-specific capabilities to access and  
184 manipulate the data may also drive the differences in needs across the PACE CoP.

### 185 3. Applications

186 A deeper look into the type of applications that use data on phytoplankton diversity (and would  
187 benefit from remote sensing data on PCC) highlights the complexities that come with defining  
188 PCC and the associated temporal, spatial, and diversity resolution. Hereafter, we present some  
189 examples of applications that range from regional to global and the level of diversity resolution  
190 associated with them.

191 Monitoring of local and regional water quality, including forecasting HABs, is a critical societal  
192 application that requires “local” knowledge and data (e.g., Lekki et al. 2019; Smith and Bernard

193 2020). Algal blooms occur in coastal and freshwater systems worldwide and include a variety of  
194 harmful species that can impact wildlife, pet, livestock, and human health (Lundholm et al. 2009;  
195 Michalak 2016). To address the need for products capable of detecting, quantifying,  
196 characterizing, classifying, and being used in forecasting applications will require finely tuned  
197 algorithms for specific HAB (or any other) algal type (Schaeffer et al. 2015, Bernard et al. 2021),  
198 at an appropriate temporal and spatial resolution to capture the transient nature of these events.  
199 PACE, similarly to the majority of heritage ocean color missions, will have adequate temporal  
200 resolution, and some limitations with regard to the spatial resolution to detect developing HABs  
201 in small water bodies. Therefore, synergies and cross-product generation with other missions  
202 with smaller spatial resolution but less optimal temporal resolution (e.g., NASA's upcoming  
203 Surface Biology and Geology (SBG<sup>5</sup>), the European Space Agency's Copernicus Hyperspectral  
204 Imaging Mission for the Environment (CHIME<sup>6</sup>), could be combined to alleviate this weakness.  
205 Lastly, low latency (i.e., the time between data collection and availability) is also critical for timely  
206 public-safety decisions in response to HABs, which requires near-real time processing of the PCC  
207 data product.

208 The fisheries industry has also increasingly integrated phytoplankton data into management  
209 activities for the purpose of: (1) fish stock assessment, (2) harvesting by identifying suitable fishing  
210 zones, and (3) fisheries management (Forget et al. 2009). The appropriate PCC definition for  
211 fisheries applications could range from single species (HABs) to more functional or taxonomic

---

<sup>5</sup> SBG stands for Surface Biology and Geology - <https://sbg.jpl.nasa.gov/>

<sup>6</sup> CHIME stands for the Copernicus Hyperspectral Imaging Mission for the Environment - [https://www.esa.int/Applications/Observing\\_the\\_Earth/Copernicus/Going\\_hyperspectral\\_for\\_CHIME](https://www.esa.int/Applications/Observing_the_Earth/Copernicus/Going_hyperspectral_for_CHIME)

212 information to support fish stock assessment and management to promote best fishing  
213 practices<sup>7</sup>.

214 At the global scale, satellite-derived PCC products can also be used to improve climate  
215 applications and research (Figure 4). Using existing satellite observations of total phytoplankton  
216 biomass, natural climate variability, such as El Niño, has been shown to directly affect  
217 phytoplankton composition, with changes trickling up the food web to the higher tropic levels  
218 (e.g., due to the change in nutrient dynamics, Fisher et al. 2015; Franz et al. 2021; McCabe et al.  
219 2016; McKibben et al. 2017; Racault et al. 2017; Rousseaux and Gregg 2012). In a similar way, PCC  
220 products can help indicate effects of the anthropogenic driven changes in aquatic ecosystems.  
221 This has been demonstrated using long term in situ datasets (e.g., Rivero-Calle et al. 2015) and  
222 models (Anderson et al. 2021; Cael et al. 2022a; Dutkiewicz et al. 2013). While prior analysis  
223 suggested natural variability compounded climate trends in current chlorophyll ocean color  
224 records (Henson et al. 2010), recent research is suggesting that ocean color itself (i.e., remote  
225 sensing reflectances) is demonstrating significant, global climate trends in 20 yearlong records  
226 (Cael et al. 2022c). PCC records from remote sensing may assist with understanding observed  
227 trends and interpreting those trends in reference to the whole ecosystem structure and role that  
228 oceanic ecosystem plays in global carbon cycle. On more local scales, in polar regions, a rapidly  
229 shifting landscape (due to the unprecedented ice loss) is modifying the local ecosystems, and  
230 composition and seasonality of phytoplankton (Eayrs et al. 2021; Meier et al. 2021; Nardell et al.  
231 2023). Understanding of such close coupling of PCC, sea ice, polar food webs, and carbon flux

---

<sup>7</sup> pezCA, an application developed by the Federación Costarricense de Pesca (FECOP) in Costa Rica, that combines policy and real time satellite based products to identify potentially favorable fishing areas, <https://pezca.org/>. pezCA team is part of the PACE early adopter program.

232 (Flexas et al. 2022; Neeley et al. 2018; Schofield et al. 2018) will benefit greatly from continuous  
233 monitoring of PCCs from space.

234 Numerical models, including simple inverse and food web models as well as more complex ESMs,  
235 provide an opportunity to integrate satellite PCC data as well as in situ data in a global context  
236 (Dinauer et al. 2022; IOCCG 2020; Siegel et al. 2023). However, data assimilation is often limited  
237 by the availability of data with appropriate units and levels of detail, such as PCC categories, and  
238 quantified uncertainties. As detailed by Le Quéré et al. (2010), not only is phytoplankton biomass  
239 (usually resolved into functional, taxonomical, and/or size groups) important for modeling  
240 applications, but so are parameters such as growth rates and export rates. Moreover, sufficient  
241 continuity of measurement (including the various seasons, see also Dutkiewicz et al. (2020)) at  
242 the global scale is required to study the feedbacks between climate and ocean biogeochemistry.  
243 Assimilation of data on PCC to improve those models will decrease uncertainty in the role of the  
244 ocean in the global carbon budget (and decrease the societal and monetary impact of such  
245 uncertainties e.g., Bontempi et al. submitted). Importantly, reported uncertainties are crucial for  
246 improving models through parametrization or data assimilation, or informing ocean color science.  
247 These uncertainties will also enable better understanding of regional, temporal bias, and  
248 instrument-based bias, especially in merged products originating from multiple instruments  
249 (Dutkiewicz et al. 2020; Gregg et al. 2017).

250 Lastly, society will have to continue to respond to the growing challenges associated with climate  
251 change. It is becoming increasingly evident that controlling future Earth warming to well below  
252 +2.0°C (preferably within +1.5°C), as is the aim of the 2016 Paris Agreement, will require  
253 deployment of large-scale technologies to reduce carbon dioxide emissions (Fuss et al. 2014; IPCC

254 2021). Several ocean-based Carbon Dioxide Removal (CDR) methods have been proposed to curb  
255 on-going global warming (GESAMP 2019; National Academies of Sciences 2022). Some of the CDR  
256 approaches that rely on the ocean, such as ocean iron fertilization or seaweed cultivation, can  
257 dramatically alter upper ocean ecosystems and phytoplankton communities (National Academies  
258 of Sciences 2022). An important part of the monitoring, reporting, and verification process of CDR  
259 will be understanding the impact of these technologies on the ocean, including the assessment  
260 of effects on PCC, net primary production, and carbon export. Remote sensing observations, such  
261 as those from PACE, will also be key to quantifying the success of ocean CDR strategies,  
262 monitoring their effects on ocean ecosystems (e.g., potential taxonomic shifts in PCC leading to  
263 harmful algal blooms), and providing data needed for ESMs to improve our understanding of the  
264 role these perturbations have on ocean ecosystems and the global carbon cycle.

#### 265 4. In situ methods

266 Many methods exist to quantify phytoplankton composition for mixed natural communities.  
267 While no individual method captures the vast diversity of marine phytoplankton across multiple  
268 dimensions (taxonomy, size, morphology, genetics, metabolism, etc.), many of these methods  
269 provide specific information that is useful to describe PCC across observations and support future  
270 PCC models. Some methods (HPLC derived pigments) have been used extensively to develop and  
271 validate satellite remote sensing approaches for PCC. Other methods (imaging-in-flow cytometry,  
272 DNA metabarcoding) offer globally distributed datasets with high taxonomic resolution that have  
273 great potential for future PACE PCC applications. Here, we review the general approaches for  
274 many common methods of phytoplankton observation and summarize their notable strengths  
275 and weaknesses, particularly with respect to remote sensing approaches (Table 2).

#### 276 4.1. Light Microscopy

277 Microscopy phytoplankton enumeration and biovolume calculation are a common approach for  
278 development and validation of ocean color PCC algorithms, especially for HAB detection (Pan et  
279 al. 2011; Soto et al. 2015; Wolny et al. 2020). In combination with cell volume to carbon models  
280 (e.g., Menden-Deuer and Lessard 2000; Worden et al. 2004), this method offers a simple route to  
281 phytoplankton carbon biomass. Standard compound and inverted microscopes are commonly  
282 used for the visualization of phytoplankton communities from water samples, offering taxonomic  
283 classification for nano- to micro size ranges in live or preserved samples (Karlson et al. 2010). The  
284 light microscopy methods used vary with size and concentration of phytoplankton within samples  
285 and on the accuracy and taxonomic resolution needed when determining PCC. A small volume of  
286 sample (1 ml or less) is suitable for counting nano- and microphytoplankton ( $>2 \mu\text{m}$ ) samples with  
287 a high concentration of cells (Godhe et al. 2007; LeGresley and McDermott 2010; McAlice 1971).  
288 However, when cells are in low concentrations or samples represent a more diverse community  
289 structure, a greater sample volume ( $<25 \text{ mL}$ ) is needed to adequately capture both small-sized  
290 and numerous cells, as well as large-sized and rare cells (Edler and Elbrächter 2010; Haas and  
291 Marshall 1989).

292 There are notable limitations to microscopic approaches. Due to the small volume of material  
293 examined for some samples, certain taxa may be over- or under-represented. Settling chamber  
294 approaches that allow for larger sampling volume and better optical resolution, resulting in a  
295 larger phytoplankton size range, are time-demanding (hours/days) in comparison to the small  
296 volume approach (minutes, Elder and Elbrächter 2010). Uncertainties in these methods can be  
297 highly variable, depending on the optical material (LeGresley and McDermott 2010), fixatives,

298 enumeration method, sample volume, and assumptions used to determine biovolume and  
299 resulting carbon content (Vuorio et al. 2007; Willén 1976). However, regardless of the approach  
300 used, the greatest limiting factors (and additional sources of uncertainty) are analyst skill level,  
301 their experience, and time required for sample analysis (see Clayton et al. 2022 and references  
302 within).

#### 303 4.2. HPLC phytoplankton pigments

304 High performance liquid chromatography (HPLC) allows for the direct quantification of a number  
305 of different phytoplankton pigments. HPLC pigments are currently one of the most widespread  
306 approaches for characterizing PCC in ocean color studies: samples have been collected  
307 throughout the global ocean, at time series observatories and along transect cruises, across  
308 depths and over seasons (e.g., Kramer and Siegel 2019; Uitz et al. 2006). HPLC methods for  
309 quantification of pigment concentrations have also been highly standardized, with successive  
310 quality control efforts to ensure consistency between measurements (Hooker et al. 2012; van  
311 Heukelem and Hooker 2011).

312 Pigment-based taxonomy is fairly low resolution and depends heavily on the HPLC pigment library  
313 used to determine PCC (e.g., Catlett and Siegel 2018). Existing methods to characterize PCC from  
314 HPLC pigments typically rely on biomarker pigments to separate phytoplankton groups based on  
315 broad taxonomic association (i.e., diatoms with fucoxanthin from dinoflagellates with peridinin)  
316 or size classes. Any pigment-based PCC method has to make necessary assumptions, as most  
317 pigments are shared between phytoplankton groups and are not unambiguous biomarkers  
318 (Jeffrey et al. 2011 and references therein). PCC methods using HPLC pigments are further  
319 complicated by environmental and physiological variations that impact pigment production and

320 expression (e.g., Catlett et al. 2022; Dierssen et al. 2015; Henriksen et al. 2002; Neeley et al. 2022;  
321 Zapata et al. 2004). Given these variations in pigment concentration and composition, statistical  
322 methods that make assumptions about constant relationships between taxa abundances and  
323 pigment ratios as well as the neglect of co-linearity among pigments must be used cautiously for  
324 evaluating PCC (e.g., CHEMTAX; Mackey et al. 1996).

325 Phytoplankton pigment absorption directly impacts the shape and magnitude of remote sensing  
326 reflectance spectra; thus, HPLC pigments are an ideal measurement for development and  
327 validation of ocean color algorithms (e.g., Chase et al. 2017; Kramer et al. 2022; Torrecilla et al.  
328 2011; Uitz et al. 2015). Studies that compare HPLC pigments with other, higher-resolution  
329 taxonomic approaches have variable success, depending on the ecosystem and the taxonomic  
330 resolution of the comparison (Chase et al. 2022; Havskum et al. 2004; Lin et al. 2019; Pan et al.  
331 2011). More comparisons between HPLC pigments and other methods using larger datasets will  
332 allow for better constraint of pigment-based PCC, and thus more accurate ocean color algorithms  
333 using PACE data.

#### 334 4.3. Flow cytometry

335 Flow cytometry (FCM) can enumerate particles and plankton from the size of viruses to cells  
336 greater than 50  $\mu\text{m}$ , depending on the instrument used and its configuration, and the whole size  
337 spectrum can be captured when combined with complementary methods (microscopy, imaging  
338 in-flow cytometry, e.g., Chase et al. 2020; Haëntjens et al. 2022). Recent evolution in FCM  
339 technology can also provide continuous or near-continuous monitoring of phytoplankton  
340 community dynamics and structure, and other ecological studies (e.g., Hunter-Cevera et al. 2021;  
341 Swalwell et al. 2011). FCM delivers cells single-file in sheath fluid past an excitation laser(s) and a

342 set of optical detectors, allowing investigators to identify specific groups of plankton based on  
343 their fluorescence and scattering properties. Additionally, some flow cytometry instruments have  
344 capability of sorting different cell types (based on their fluorescence and scattering properties) in  
345 separate streams, allowing for more detailed analysis (e.g., phytoplankton group specific carbon  
346 content, Graff et al 2012; Casey et al. 2013). Samples can be run “live” or preserved (Lepesteur et  
347 al. 1993). Published relationships can then be used to convert cell size (in  $\mu\text{m}$ ) to cell biovolume  
348 (e.g., Calvo-Díaz and Morán 2006) and carbon (e.g., Menden-Deuer and Lessard 2000; Worden et  
349 al. 2004). Fluorescence emission from the excitation of pigments can be used to distinguish  
350 specific phytoplankton populations for some groups, such as the pico-sized cyanobacteria  
351 *Synechococcus*, which produces an orange fluorescence signal when the phycoerythrin in the cell  
352 is excited by a blue laser, distinguishing them from other small cells (Olson et al. 1988).  
353 Fluorescent dyes may also be used to enumerate different groups of cells without specific marker  
354 pigments (Rose et al. 2004).

355 Uncertainty in PCC data from FCM can come from both the sample collection and data analysis.  
356 Studies have shown that fixatives can impact the autofluorescence signal or cause cell loss and  
357 cell shrinkage by phytoplankton cells if samples are stored for long periods of time, e.g., >1 month  
358 (Marie et al. 2014; Sato et al. 2006; Vaultot et al. 1989). The instrument calibration method  
359 determines the model used to derive cell size from fluorescence or scattering. Uncertainties also  
360 arise during data analysis when discrete populations of cells are separated (sometimes  
361 subjectively by operator) based on fluorescence and scattering parameters. Nevertheless, FCM is  
362 an effective approach that can provide enumeration of pico and nano-sized cells, which are

363 important, novel datasets that support development of PCC algorithms (e.g., Lange et al. 2020;  
364 Kramer et al. 2020; Thyssen et al. 2015).

#### 365 4.4. Imaging-in-flow cytometry

366 Imaging-in-flow instruments have revolutionized collection and analysis of aquatic samples for  
367 the qualification and quantification of PCC. These approaches combine flow cytometric  
368 enumeration with the digital photography of particles that can be used for taxonomic  
369 identification. A number of different imaging-in-flow instruments, such as the Imaging Flow  
370 Cytobot (Olson and Sosik 2007), Underwater Vision Profiler (UVP, Picheral et al. 2010), and  
371 FlowCAM (Sieracki et al. 1998), have been developed over the last two decades and capture  
372 different regions of the size spectrum (Lombard et al. 2019). Unlike standard microscopy, these  
373 instruments allow for automated, rapid collection of plankton and particle images over high  
374 spatial and temporal resolution that can be classified and enumerated (sometimes iteratively)  
375 after collection using image recognition by machine learning.

376 An imaging in-flow system typically contains an objective, an excitation laser, and fluorescence  
377 detectors to detect *Chl a* fluorescence and light scatter. A water sample is drawn through a flow  
378 cell and past the optical package, where particles that are excited by the laser get magnified by  
379 the objective (like a microscope) and imaged by a color or monochrome camera. The images are  
380 interpreted based on morphological characteristics and/or size dimensions that may be used by  
381 a machine learning classifier or manually attributed to specific types of particles, plankton, or  
382 phytoplankton. As with every method, there are challenges that must be considered. Imaging-in-  
383 flow systems typically measure the larger range of phytoplankton (e.g.,  $>6\mu\text{m}$  for the IFCB). The  
384 large number of images that are collected creates challenges regarding the time needed to

385 complete automated and manual classification, and in the interpretation and sharing of results  
386 (Durden et al. 2017; Kerr et al. 2020). Advances in machine learning techniques and other  
387 automated approaches (Orenstein et al. 2022), in particular deep learning such as convolutional  
388 neural networks, will increase the accuracy of automated classifications and reduce the analysis  
389 time, thereby increasing throughput of PCC data. The scientific and environmental monitoring  
390 communities using these methods are coming together to overcome these challenges not only  
391 for image post-processing, but also dataset creation and taxonomic training augmentation  
392 (Clayton et al. 2022, Neeley et al. 2021). Overall, imaging-in-flow methods present great potential  
393 for describing PCC in situ, particularly for PACE applications, given the relative ease of sampling  
394 and high taxonomic resolution.

#### 395 4.5. DNA metabarcoding

396 Numerous molecular approaches are available to quantify phytoplankton diversity, population  
397 dynamics, and PCC (Johnson and Martiny 2015). DNA meta-barcoding is now one of the most  
398 widely used methods to provide a holistic view of PCC including diverse members of the  
399 phytoplankton community. DNA meta-barcoding refers to targeted amplicon sequencing of  
400 highly conserved, hypervariable “barcode” genes. These data are usually compositional (i.e.,  
401 estimate proportions rather than concentrations or counts), which complicates analysis and  
402 interpretation of PCC (Aitchison 1982; Gloor et al. 2017), but some exciting approaches have been  
403 developed recently to remove this constraint (Lin et al. 2019; Satinsky et al. 2013).

404 The taxonomic resolution of DNA meta-barcoding varies from division- to species-level depending  
405 on a number of factors including the analysis workflow or the specific Amplicon Sequence  
406 Variants (ASV). Uncertainty in relative sequence abundances is introduced by both wet lab and

407 bioinformatic procedures and is difficult to quantify (Catlett et al. 2020; Yeh et al. 2021). In  
408 general, nucleic acid sequencing data are generated through a series of complex biochemical  
409 reactions that make it difficult to evaluate and constrain analytical uncertainty. Consistent use of  
410 positive and negative controls to ensure reproducibility in sequence analysis has only recently  
411 become common practice (Bradley et al. 2016; Parada et al. 2016), but is still omitted by many  
412 investigators. Interpretation of relative (or absolute) sequence abundances is not straightforward  
413 in practice, as the number of barcode gene copies per cell or unit biomass can vary across taxa  
414 depending on the chosen barcode gene (Gong and Marchetti 2019; Zhu et al. 2005). Despite these  
415 caveats, several recent studies have demonstrated that DNA meta-barcoding workflows can  
416 provide accurate and precise estimates of the relative sequence abundances of most  
417 phytoplankton (Catlett et al. 2020; Yeh et al. 2021). Some barcode genes also provide relative  
418 sequence abundances that scale roughly with cell size, biovolume or biomass proportions (de  
419 Vargas et al. 2015; Godhe et al. 2008; Zhu et al. 2019).

420 DNA meta-barcoding data have not been employed in direct validation of satellite algorithms to  
421 the best of our knowledge, but these studies suggest high potential for their use in efforts to  
422 validate the next generation of PCC algorithms developed for PACE (Catlett et al. 2022). Despite  
423 some methodological challenges, the ability to sample a nearly comprehensive range of size  
424 classes, the detailed resolution of taxonomic and functional diversity, and the growing  
425 appreciation for the quantitative potential of well-validated nucleic acid sequencing workflows  
426 make these methods primed for in situ PCC quantification.

#### 427 4.6. Phytoplankton optics

428 Phytoplankton, either due to their size, or morphological (external or internal) characteristics  
429 have a taxa-specific contribution to the scattering of the light in the water column (Organelli et  
430 al. 2018; Poulin et al. 2018; Stramski et al. 2001; Stramski and Kiefer 1991; Whitmire et al. 2010),  
431 and that signal is present in the  $R_{rs}(\lambda)$  as well. Ocean color measurements can provide rudimentary  
432 estimates of the slope of the particulate backscattering or particulate attenuation spectra  
433 through the inversion of  $R_{rs}(\lambda)$  (e.g., Roesler and Boss 2003; Loisel et al. 2018). Particulate  
434 backscattering itself, which is readily retrievable from in situ or satellite derived  $R_{rs}(\lambda)$  (e.g.,  
435 Werdell et al. 2013) can be used to infer phytoplankton size composition (Kostadinov et al. 2022).  
436 Backscattering can be affected by internal and external morphological characteristics that impact  
437 the shape of the slope (see Organelli et al. 2018), whereas particulate attenuation is mostly  
438 dependent on particle size. Increased values of attenuation spectral slope are associated with  
439 particle populations that have higher proportions of smaller size particles, whereas the inverse is  
440 true for backscattering slopes (e.g., Boss et al. 2001). This approach is highly applicable to the  
441 open ocean where changes in particle population are driven by PCC change and could offer an  
442 additional dimension in information when distinguishing the phytoplankton with different  
443 mineral components (such as silica and calcium carbonate).

444 Absorption of the phytoplankton is to the first extent driven by the pigments present in the cell.  
445 Chlorophylls, and other (sometimes taxa-specific) cellular pigments (see 4.2 and references  
446 therein) determine the shape of the absorption spectra (Mobley 2022 and references within).  
447 Additionally, pigment packaging and the structure of protein-pigment complexes will have a  
448 significant effect on the phytoplankton absorption spectra. Shape, peak, and width of the specific

449 absorption features can be used as a tool to detect different taxa from in situ measurements of  
450 absorption (e.g., Chase et al. 2013). While some of these features (e.g., Chlorophyll peaks) are  
451 visible in  $R_{rs}(\lambda)$  and therefore easy to relate to pigment concentrations, ocean reflectance  
452 inversion models (e.g., GIOP – Werdell et al. 2013) are often used to derive phytoplankton  
453 absorption from the  $R_{rs}(\lambda)$ , that is ultimately used to infer PCC distribution.

## 454 5. Phytoplankton composition from space

### 455 5.1. Heritage multispectral PCC remote sensing algorithms

456 Heritage approaches for deriving phytoplankton composition from ocean color typically exploit  
457 relationships generated from pairing in situ phytoplankton data with either in situ  $R_{rs}(\lambda)$  or top-  
458 of-atmosphere (TOA) satellite radiometry. Until recently, satellite and in situ radiometry  
459 measurements were mostly collected at multispectral resolution. Therefore, the methods  
460 developed to derive PCC relied on the multispectral information ( $R_{rs}(\lambda)$ ) and could be applied to  
461 SeaWiFS, MODIS, and multispectral ocean color missions operated by other space agencies  
462 (Alvain et al. 2005; Alvain et al. 2008; Ben Mustapha et al. 2014; Sathyendranath et al. 2004;  
463 Werdell et al. 2014; Westberry et al. 2005). In general, their applicability and success (and  
464 associated uncertainties) depend heavily on the in situ training datasets and the formulated  
465 methodology. Recent reviews have demonstrated that existing ocean color PCC approaches agree  
466 on a global scale, but disagree considerably on regional scales (e.g., Bracher et al. 2017; IOCCG  
467 2014; Kostadinov et al. 2017; Mouw et al. 2017). These reviews also identified numerous gaps in  
468 ocean color-based PCC (including mismatch between in situ, satellite and model data, the lack of  
469 uncertainty estimates for the satellite data, and the spectral limitation of existing sensors) that  
470 advanced ocean color missions such as PACE will be able to address. Looking towards PACE ocean

471 color and polarimetry data, we can draw from the knowledge gained from these previously  
472 developed methods, which address global-scale data products as well as more regional taxon or  
473 phytoplankton group specific products.

474 The breadth of methods for detecting PCC from space includes approaches that rely on total  
475 biomass (e.g., Hirata et al. 2011), or other proxies for abundance, rather than spectral shape or  
476 features, as well as methods that rely on single or multiple ocean color products;  $R_{rs}(\lambda)$ , carrying  
477 information from both scattering and absorption components (e.g., Morel and Prieur 1977; Xi et  
478 al. 2021); phytoplankton absorption (Brewin et al. 2011b; Bricaud et al. 2007 and similar, derived  
479 from  $R_{rs}(\lambda)$  via semi analytical models such as Werdell et al. 2013); or backscattering (Kostadinov  
480 et al. 2009). Different mathematical and statistical approaches (e.g., Gaussian decomposition,  
481 principal component analysis, derivatives, machine learning etc.) have been used to extract the  
482 information on PCCs from the abovementioned datasets. A more comprehensive list of  
483 algorithms is presented in Table 3. The types of PCC retrievals that result from previously  
484 developed methods are highly variable. Certain algorithms focus on the retrieval of single taxa,  
485 while others retrieve multiple taxa or fractional contributions of multiple taxa. These retrievals  
486 are generally reported as probability of detection, as the dominating portion of biomass (usually  
487 *Chl a*), as the proportion of the total *Chl a* concentration, or in concentration units such as biomass  
488 (e.g., cells) per volume. In contrast, phytoplankton size classes (PSCs) are used to define the  
489 heterogeneity in size distribution of phytoplankton communities; mainly reporting three size  
490 classes: the pico-, nano-, and microphytoplankton (<2  $\mu\text{m}$ , 2-20, and >20  $\mu\text{m}$ , respectively). Some  
491 approaches rely on the backscattering to retrieve PSCs, and in combination with modeling,  
492 retrieve the particulate and phytoplankton size distribution, expressed as % of total biomass or

493 total phytoplankton carbon (Kostadinov 2016; Kostadinov et al. 2022). Other methods estimate  
494 the contributions of each of these three classes to total *Chl a*, through assigning HPLC-determined  
495 accessory pigments to taxonomic groups, and the groups to size classes (as per Vidussi et al. 2001,  
496 Uitz et al. 2006). Numerous revisions and evaluations of the “Diagnostic Pigment Analysis”  
497 approach to estimating PSCs from accessory pigment concentrations have been published and  
498 provide a body of literature for reference regarding the development and validation of PSC  
499 algorithms from space. Ultimately, these accessory pigments themselves can be used to estimate  
500 PCC (Table 3).

501 Identification of phytoplankton composition down to the species level is possible in some cases  
502 for certain taxa with unique optical properties. One example is the cosmopolitan coccolithophore  
503 species *Emiliana huxleyi*, which when present at high concentrations (blooms) in the surface  
504 layer, can profoundly impact the optical properties of the upper ocean (Balch et al., 1991; Balch,  
505 2018). This detection is not based on the absorption properties of the phytoplankton, but rather  
506 on its intense scattering properties (Neukermans and Fournier, 2018), which lead to “milky white”  
507 seas observable even in broadband satellite sensors like AVHRR (Loveday and Smyth, 2018).  
508 Similarly, algorithms have been developed to detect the blooms of dinoflagellate *Karenia brevis*  
509 due to its consistently lower backscattering properties compared to other types of blooms found  
510 in the same region (Craig et al., 2006; Cannizzaro et al., 2008; Soto et al., 2015). The addition of  
511 vacuoles or intracellular spaces that create high scattering also has a substantial effect on  $R_{rs}(\lambda)$   
512 even at relatively low biomass and has led to approaches for discerning cyanobacteria (Matthews  
513 et al., 2012; Matthews and Bernard, 2013, Schaeffer et al. 2015). Combination of increased  
514 scattering due to the intercellular gas vesicles and pigment specific signal in  $R_{rs}(\lambda)$  was the base

515 of early algorithms used to detect cyanobacteria *Trichodesmium* from space (Subramaniam et al.  
516 2001; Subramaniam and Carpenter 1994). More recent approaches rely on the dense surface  
517 accumulations (sea slicks, Hu et al. 2010; McKinna et al. 2011), or rely on *Trichodesmium* specific  
518 bio-optical properties (Dupouy et al. 2011; Westberry et al. 2005; see review in McKinna 2015).

## 519 5.2. Anticipated benefits of the PACE instruments

### 520 5.2.1. Hyperspectral ocean color

521 Hyperspectral  $R_{rs}(\lambda)$  from PACE will provide, by definition, additional information content over  
522 existing multispectral data and their associated algorithms. Several studies have addressed  
523 optimal spectral resolutions and/or band placement for radiometric measurements, starting with  
524 work from Lee et al. in 2007. Wolanin et al. (2016) demonstrated that band placement  
525 requirements depend on both the method as well as the target phytoplankton groups to be  
526 retrieved, and they suggest that hyperspectral (vs. any lower spectral resolution) observations  
527 are ideal. Torrecilla et al. (2011) used field data of concurrent phytoplankton absorption and  
528 remote-sensing reflectance measurements and demonstrated the advantage of high-spectral  
529 resolution data over multi-spectra data for discriminating phytoplankton pigment assemblages in  
530 open ocean, including the benefits of spectral derivative analysis. Vandermeulen et al. (2017),  
531 used a database of in situ hyperspectral reflectance measurements from a wide range of water  
532 types to demonstrate that a spectral interval of 5 nm is optimal to separate differently absorbing  
533 phytoplankton groups while also accounting for measurement uncertainties. Further, Kramer et  
534 al. (2022) found a similar result where the performance of statistical models for predicting  
535 phytoplankton pigment concentrations was greatly reduced above a spectral interval of 5 nm.  
536 Hence, PACE radiometry can be used to separate the contribution or fine scale spectral features

537 of phytoplankton and large-scale spectral features of the other oceanic constituents (>100 nm,  
538 e.g., CDOM, backscattering) as recently demonstrated by Kramer et al. (2022).

539 Hyperspectral phytoplankton absorption and  $R_{rs}(\lambda)$  spectra are more effective than multispectral  
540 data during derivative, Gaussian, and clustering analyses for pigment assemblage discrimination  
541 and size-based, phytoplankton community composition assessment (Chase et al. 2017; Kramer et  
542 al. 2022; Lange et al. 2020; Roelke et al. 1999; Torrecilla et al. 2011; Uitz et al. 2015). This finding  
543 reflects the relative similarity of spectral absorption of different phytoplankton pigments and  
544 groups (e.g, Garver et al. 1994; Mao et al. 2010), which necessitates the use of optical information  
545 at a high spectral resolution to discern subtle differences in spectral absorption and reflectance  
546 that are the result of differently absorbing phytoplankton pigments. By focusing on changes on  
547 small spectral scales some of these approaches minimize the source of noise in absolute signals  
548 (usually associated with atmospheric correction approaches – see Ibrahim et al. 2018).

549 Existing algorithms that take advantage of hyperspectral  $R_{rs}(\lambda)$ , have demonstrated their  
550 capability on data collected by previously flown hyperspectral instruments; either by quantifying  
551 *Chl a* or phytoplankton absorption to specifying taxonomic groups. Studies based on the  
552 Hyperspectral Imager for the Coastal Ocean (HICO) (Lucke et al. 2011) have successfully  
553 demonstrated the use of hyperspectral  $R_{rs}(\lambda)$  to observe a phytoplankton bloom in Monterey Bay,  
554 CA (Ryan et al. 2014), to differentiate a red tide ciliate bloom (*Mesodinium rubrum*) in Long Island  
555 Sound, NY at high spectral and spatial resolution using unique yellow fluorescence features  
556 (Dierssen et al. 2015), and to map PCC in coastal China using machine/transfer learning approach  
557 (Zhu et al. 2019). Recent publications have also shown high-quality retrievals of *Chl a*,  
558 phycocyanin, and phytoplankton absorption spectra from HICO imagery over freshwater and

559 coastal ecosystems (Gitelson et al. 2011; O'Shea et al. 2021; Pahlevan et al. 2021), and  
560 discrimination of cyanobacteria monospecific blooms in large (Wynne et al. 2008) and small lakes  
561 (Kudela et al. 2015). In the open ocean, the PhytoDOAS method, which makes use of  
562 hyperspectral  $R_{rs}(\lambda)$ , has been applied to SCIAMACHY (SCanning Imaging Absorption  
563 spectroMeter for Atmospheric Chartography) to discern blooms of cyanobacteria,  
564 coccolithophores, and diatoms (Bracher et al. 2009; Sadeghi et al. 2012).

565 The OCI on PACE will be able to measure ultraviolet (UV) wavelengths at the same high spectral  
566 resolution as the visible portion of the spectrum. Information from the UV part of the ocean  
567 color signal will bring additional means to constrain the phytoplankton community structure.

568 Numerous phytoplankton species produce specific MAAs of individual spectral characteristics  
569 (Llewellyn and Airs 2010), with additional UV absorbing compounds (Jeffrey et al. 1999) that  
570 could impact the remote sensing reflectance and be traced back to either species composition  
571 or community-specific response to environmental conditions (e.g., polar regions, Ha et al. 2018).

572 Using in situ measured  $R_{rs}(\lambda)$  Kahru and Mitchell (1998) demonstrated that the presence of a  
573 HAB species, *Lingulodinium polyedra* could be distinguished from diatom-dominated  
574 populations by the absorption of Mycosporine-like amino acids (MAAs), compounds produced  
575 by dinoflagellates to protect organelles from harmful UV rays. This approach was recently  
576 validated using a UV band from JAXA's GCOM-C satellite to track the spatial and temporal  
577 distribution of this specific HAB (Kahru et al. 2021).

#### 578 5.2.2. Polarimetry

579 PACE will carry two polarimeters, HARP2 and SPEXone, targeting atmospheric properties.  
580 Measurements of atmospheric properties by these instruments will indirectly advance the

581 retrieval of PCC from hyperspectral OCI information by improving atmospheric correction through  
582 better characterization of aerosols. Regarding the measurement of oceanic properties, these  
583 instruments are limited by their mode of operation; collecting information on coarser spatial  
584 resolution (3-4 km vs 1 km for OCI) and measuring approaches that maximize the number of  
585 scattering angles. However, a similar instrument, ESA's POLDER (Polarization and Directionality  
586 of the Earth's Reflectances), has been previously used in combination with modeling to offer  
587 information about characteristics of oceanic bulk particle composition (Loisel et al. 2008). Similar  
588 approaches could be used to derive additional information from PACE's polarimetric data,  
589 separating organic from inorganic particles, inferring particle size distribution and other particle  
590 properties that can be used in better retrievals of PCC and constrain uncertainties associated with  
591 phytoplankton products (see Jamet et al. (2019) and references within). However, it is important  
592 to note the basic need to first better understand the Muller matrix (i.e., inherent polarization  
593 properties) of different marine particles/phytoplankton as a prerequisite to potential meaningful  
594 interpretation and use of polarization properties of natural light fields, such as polarized water-  
595 leaving light derived from PACE's polarimeters.

### 596 5.3. Other approaches to deriving PCC from space

597 In addition to the development of PCC algorithms that solely rely on optical properties of  
598 phytoplankton, the scientific community has developed various approaches that use non-optical  
599 proxies including model outputs or results from analysis of lower-level data (e.g., variables  
600 derived from multiple measurements<sup>8</sup>) to derive PCC. These data are referred to as Level-4 data  
601 products and include satellite-based models, machine learning approaches that could incorporate

---

<sup>8</sup> earthdata.nasa.gov

602 ancillary data, and Earth System Models. Such approaches have the advantage of being able to  
603 integrate in situ, model, and/or satellite data to gain insights that would not be achievable with  
604 the use of phytoplankton optical properties alone and can provide information on variables that  
605 might not currently have designated algorithms (e.g., Anderson et al. 2009; Hill et al. 2020).

606 Several satellite-based models have emerged over the years that result in phytoplankton  
607 taxonomic composition as well as phytoplankton size information (e.g., Xi et al. 2021). Hirata et  
608 al. (2011), for example, used satellite *Chl a* to derive the fraction of both phytoplankton  
609 composition and size fraction. California Harmful Algae Risk Mapping (C-HARM) is routinely (since  
610 2014) using a combination of multispectral  $R_{rs}(\lambda)$ , remote sensed *Chl a*, sea surface temperature  
611 and ROMS modeling to forecast distribution of *Pseudo-nitzschia* spp. and associated toxins  
612 (Anderson et al. 2019). By combining hyperspectral in situ  $R_{rs}(\lambda)$  and sea surface temperature in  
613 a principal component analysis framework, Lange et al. (2020) derived cell counts for several  
614 smaller phytoplankton groups across the Atlantic, demonstrating improved performance for such  
615 a combined approach over a multispectral one (Figure 5).

616 Machine learning approaches to estimate phytoplankton composition have also been developed  
617 in the last decades. Raitzos et al. (2008) developed an artificial neural network that incorporates  
618 ecological and geographical information (e.g., longitude, latitude, season) with ocean color  
619 products (e.g., *Chl a*, normalized water-leaving radiance, PAR), bio-optical characteristics, and  
620 remotely sensed physical parameters (e.g., SST, wind stress). Using this approach, they were able  
621 to discriminate four major phytoplankton functional types based on probability of occurrence  
622 (diatoms, dinoflagellates, coccolithophores, and silicoflagellates) with an accuracy of more than  
623 70%. Palacz et al. (2013) used another approach that relies on an artificial neural network to

624 simulate the global distribution of PCC with a focus on diatoms and coccolithophores in the high  
625 nutrient low chlorophyll (HNLC) regions. A recent approach by Chase et al. (2022) utilizes *Chl a* in  
626 combination with environmental variables (sea surface temperature and salinity) to retrieve  
627 diatom carbon biomass in the North Atlantic. This approach is a clear demonstration of  
628 improvement in PCC retrieval due to the inclusion of environmental variables as well as imaging  
629 in-flow cytometry data to define PCC during algorithm development (Figure 6). These approaches  
630 become even more relevant in coastal and freshwater systems where phytoplankton absorption  
631 features in  $R_{rs}(\lambda)$  are masked by strong absorption and backscattering by other optically relevant  
632 constituents, hence, auxiliary environmental and physical information could further constrain the  
633 solution space enabling high-quality PCC retrievals.

634 Finally, ESMs integrate in situ and satellite data through parametrization, forcing, and/or  
635 assimilation. ESMs can provide global coverage (no gaps due to high solar zenith angle, clouds,  
636 polar night, etc.) and can provide information on components of the ocean biogeochemical cycle  
637 that cannot currently be derived from satellite data alone (IOCCG 2020). These models do  
638 encompass the diversity of phytoplankton as either functionality (e.g., diatoms, cyanobacteria,  
639 diazotrophs, etc; Bopp et al. 2005; Gregg and Casey 2007) or size classes (e.g., Ward et al. 2012;  
640 Ward and Follows 2016). ESMs make assumptions that are aligned with our current  
641 understanding of phytoplankton dynamics (i.e., nutrient uptake, growth rate, sinking rate etc.).  
642 Some models also assimilate satellite ocean color products (e.g., Gregg and Casey 2007; Jones et  
643 al. 2016; Shulman et al. 2013) in models including PCC as functional groups (e.g., Ciavatta et al.  
644 2018; Skákala et al. 2018) or size classes (e.g., Xiao and Friedrichs 2014).

#### 645 5.4. Challenges of deriving PCC from space

646 In the previous sections, we highlighted approaches that are currently used to detect the  
647 dominant phytoplankton groups in the world aquatic ecosystem from ocean color imagery. In  
648 vast areas of open ocean, non-phytoplankton particles (i.e., detritus, heterotrophic bacteria) are  
649 more abundant than phytoplankton. While all these particulate (and dissolved) components of  
650 the open oceanic systems contribute to the ocean color, the strong absorption by phytoplankton  
651 pigments dominates the contribution to the ocean color signature, which has been identified as  
652 a promising signal in terms of identifying groups of phytoplankton (Alvain et al. 2008; Devred et  
653 al. 2006). As algal particle concentrations increase, however, scattering by phytoplankton can  
654 dominate the phytoplankton absorption properties and therefore lead to inaccuracies in  
655 measured optical properties (Brewin et al., 2017). As demonstrated by Garver et al. (1994) both  
656 pigment assemblages and pigment packaging effects (self-shading effect in large cells) contribute  
657 to the observed similarities in absorption spectra among phytoplankton, making it challenging to  
658 differentiate between different species solely based on their spectral characteristics. They found  
659 that more than 99% of the variance in the particulate absorption spectra was related to the  
660 biomass, and less than 0.5% was related to the presence of auxiliary pigments (Garver et al.,  
661 1994). The combined effects of assemblage effective cell diameter and phytoplankton biomass,  
662 together with non-algal optical contributors, are not easily interpreted from  $R_{rs}(\lambda)$  as these  
663 quantities have ambiguous effects on the bulk optics (Evers-King et al., 2014). Recent information  
664 content studies have shown that the spectral signatures of absorption by different phytoplankton  
665 groups are similar within the uncertainty of the measurement mainly because of the considerable  
666 overlap in pigment composition, and thus spectral absorption, between different groups spatially

667 and temporally across aquatic ecosystems (Cael et al. 2020). Also, correlation among reflectances  
668 can decrease information content in hyperspectral data, limiting the capability of derivation of  
669 independent parameters (Cael et al. 2022b).

670 Using the hyperspectral reflectance spectra from UV to NIR (320 to 715 nm) incorporates  
671 significantly more information (than traditional multispectral) including backscattering of the  
672 phytoplankton and associated particles, as well as fluorescence information, and may yield  
673 further taxonomic resolution. New methods to differentiate fractional phytoplankton  
674 composition from reflectance detected six different groups globally including diatoms,  
675 dinoflagellates, haptophytes, green algae, prokaryotes, and *Prochlorococcus* (Xi et al. 2020).  
676 However, such approaches may not apply to all coastal and inland waters. In the North Sea,  
677 Castagna et al. (2021) found that blooms of *Phaeocystis globosa* are synchronous with those of  
678 the diatom *Pseudo-nitzschia delicatissima*, both harmful bloom-forming species with similar  
679 pigmentation and optical properties.

680 Remote sensing algorithms and biogeochemical models can be derived and tuned for the regional  
681 or local phytoplankton groups down to specific taxa, if they are known to occur in an area and do  
682 not have similar optical properties compared to other local taxa (examples listed in chapter 5.1  
683 and Table 3). For example, in South African waters, five different probabilistic indicators of  
684 harmful algal blooms were retrieved relevant to the aquaculture industry including waters with  
685 high and low density of dinoflagellate, *Pseudo-nitzschia* dominated waters, as well as waters with  
686 mixed assemblages of high and moderate concentrations (Smith and Bernard 2020). We have  
687 only begun to assess the hyperspectral scattering and fluorescence properties that may also aid  
688 in differentiating different types and stages of blooms, as well as relationships to seasonal trends

689 and other remotely sensed quantities including polarization parameters, temperature,  
690 photosynthetically available radiation, and salinity (see Section 4.2.3).

691 Some studies have developed hyperspectral techniques to differentiate over 20 different species  
692 of phytoplankton (e.g., Zhu et al., 2019). While the statistical approaches used in such studies are  
693 robust, the lack of validation data across the breadth of space and time hinders the widespread  
694 application of such tuned approaches. Our approach to treatment of error and uncertainties in  
695 these applications determines the difference between retrieving four to five phytoplankton  
696 groups rather than >60 (Cael et al. 2020). A recent study using a large HPLC pigment dataset  
697 confirmed that only a limited number of phytoplankton groups (~4) may be differentiated globally  
698 including cyanobacteria, diatoms/dinoflagellates, haptophytes, and green algae (Kramer and  
699 Siegel 2019). However, they also demonstrated that, on regional scales, pigment association  
700 varies, suggesting that regional algorithms could resolve up to 6 taxonomic groups. Data from the  
701 Santa Barbara Channel, California revealed that around five phytoplankton pigment communities,  
702 which are covarying assemblages of phytoplankton groups, could be differentiated based on their  
703 spectral properties (Catlett and Siegel, 2018; Catlett et al., 2021).

704 Another challenge of deriving PCC from space is that the vertical structure of phytoplankton in  
705 the ocean is not always homogenous as many of the models are assuming; phytoplankton layers  
706 are often found across the oceanic ecosystems. Depth on which specific phytoplankton is, as well  
707 as a thickness and number of layers with different PCCs will heavily influence observed  $R_{rs}(\lambda)$  at  
708 the surface, as that signal represent optically weighted contribution of all components. These  
709 vertical distributions are not simple to resolve either from perspective of total biomass (Gordon  
710 and McCluney 1975; Morel and Berthon 1989; Stramski and Stramska 2005), fluorescence signal

711 (Erickson et al. 2019) size structure (Uitz et al. 2006), or PCC (Lange et al. 2018; Werdell et al.  
712 2014).

713 Another challenge requiring attention is the mismatch in the products that some of the remote  
714 sensing PCC approaches produce and in situ measurements. Above mentioned approaches that  
715 output % of biomass (chlorophyll or carbon) to specific size class or group, are hard to validate,  
716 as in situ datasets for those parameters are rare, or modeled (carrying lot of assumptions,  
717 therefore errors), or unavailable. In those situations, validation is carried through comparison  
718 with in situ measurements that explain PCC in different units (see section 4), leading to additional  
719 uncertainties that are often unaccounted for. Furthermore there is a spatial and temporal  
720 mismatch between in situ and remote sensing data. The current approach, where a 5×5 pixel  
721 (nominally) box is centered on a pixel closest to an in situ data point, has shown success at  
722 validating indices of total phytoplankton biomass on open ocean scales. A key reason for this is  
723 the high dynamic range of *Chl a* concentration (and by proxy, total phytoplankton biomass) in the  
724 ocean, which may not be the case for individual phytoplankton taxonomic groups. Issues of sub-  
725 pixel variability, however, are not trivial in heterogeneous and dynamic ocean regions, including  
726 coastal areas that are likely to have strong tidal influences, river runoff, stratification, sediment  
727 resuspension, and other biophysical interactions that create patchy water mass distributions  
728 (e.g., Aurin et al. 2013; Ryan et al. 2005). In addition, diel variability in phytoplankton processes  
729 causes changes in cell size consistent with patterns of cell growth during the light period and cell  
730 division late in the day (Sosik et al. 2003) that is visible in optical properties, including  $R_{rs}(\lambda)$  (e.g.,  
731 Briggs et al. 2018; Claustre et al. 2002; Concha et al. 2019; Gernez et al. 2011; Henderikx Freitas  
732 et al. 2020; Poulin et al. 2018; Stramski et al. 1995; Stramski and Reynolds 1993). In regions with

733 considerable spatiotemporal variability, for example, matching the seasonal climatology can be a  
734 useful tool to evaluate and validate different algorithms (Henderikx Freitas and Dierssen 2019).  
735 Going forward, thoughtful approaches that take in consideration the spatiotemporal variability  
736 of PCC, phytoplankton growth stages, and associated bio-optical retrievals should be applied to  
737 the validation of these remote sensing products.

## 738 6. Phytoplankton from PACE

739 In this review we presented a three-pronged approach to define PCC from PACE; as information  
740 that is needed by the users, definable by in-situ methodology, and detectable from satellites  
741 (Figure 7). In the preceding sections we defined current capabilities to resolve phytoplankton  
742 taxonomy from in situ and space-based observations. We described the strengths and  
743 weaknesses of each approach. We also described the availability of various techniques for  
744 phytoplankton enumeration and identification, from pigments to DNA to microscopy to imaging  
745 in flow approaches. The current suite of satellite PCC algorithms is largely only capable of deriving  
746 size classes, with a few that can discriminate unique taxonomic classes. Now the question is: what  
747 is possible with PACE? Although we would like to satisfy every user's needs, we must be realistic  
748 in our assumptions or expectations, and limitations that are outside of the sphere of technological  
749 capabilities of PACE instruments and our methods in-situ.

### 750 6.1. In situ data requirements

751 Even with PACE's technological advancements, its potential to characterize the phytoplankton  
752 community will still depend on the availability of pigment and taxonomic data—that is, how well  
753 PCC is assessed in situ and subsequently used in algorithm development and validation.  
754 Previously, most PCC algorithms developed for application to satellite data have relied on

755 phytoplankton accessory pigment concentrations to define the phytoplankton groups of interest.

756 A challenge arises in that the biomass of a given phytoplankton group cannot be directly defined

757 using accessory pigment concentrations, as there are assumptions and approximations made

758 when defining groups via pigment proxy (Jeffrey et al. 2011). Diversifying the types of in situ data

759 used to define PCC (see Section 4) as well as use of multiple types of in situ taxonomic approaches

760 will not only will improve the development of robust PACE PCC algorithms, but it will be critical

761 as we go forward, as each data type has its advantages and limitations (see Catlett et al. 2022).

762 Additionally, the limited number of validation exercises have been ad-hoc, and to ensure the

763 quality and fidelity of the PCCs produced from PACE, validation must be done in a continuous

764 standardized fashion (PACE mission 2020).

765 The first steps for validation of PACE algorithms will be using solid foundation built upon heritage

766 ocean color missions such as SeaWiFS, MODIS, MERIS, and VIIRS. From these missions, we have

767 learned that the development, usability, and reliability of ocean color data depends on the

768 availability of quality field data from (and prior to) launch date through the final days of the

769 mission. Here we define “quality field data” as that which have been collected and processed

770 following vetted community protocols, and deposited in an open access long-term data

771 repository, especially those following up-to-date international data standards. The need for

772 calibration and validation of optical oceanographic data during the SeaWiFS era set the stage for

773 development of the SeaWiFS Bio-optical Archive and Storage System (SeaBASS), which today is

774 one of the largest data repositories for optical oceanographic data. SeaBASS is part of NASA's

775 Ocean Biology Distributed Active Archive Center (OB.DAAC), operating under NASA's Earth

776 Observing System Data and Information System (EOSDIS). In addition to serving the ocean color

777 community as a long-term data repository and data distribution (via OB.DAAC), SeaBASS is  
778 responsible for compiling and curating data used for calibration and validation activities of ocean  
779 color satellite missions, including PACE. Most of the radiometric and bio-optical data used for  
780 validation is shared via NASA NOMAD (NASA bio-Optical Marine Algorithm Dataset), which is a  
781 publicly available, global, high-quality in situ bio-optical data set for use in ocean color algorithm  
782 development and satellite data product validation activities.

783 When it comes to measurements of phytoplankton and community composition, SeaBASS has  
784 been primarily limited to phytoplankton pigments and relatively few flow cytometry and imaging  
785 datasets. As HPLC based *Chl a* has historically been the preferred validation data type for ocean  
786 color *Chl a*, community has developed standard protocols, and has participated in numerous  
787 round robin comparisons, that allowed standardization of not only *Chl a*, but the whole HPLC  
788 pigment suite across international community (e.g., SeaHARRE round robin series, Hooker et al.  
789 2012). In preparation for PACE and to expand phytoplankton data availability beyond pigments,  
790 SeaBASS implemented community protocols outlined in Neeley et al. (2021) for standardizing  
791 image data collected using imaging-in-flow instruments, such as the IFCB, UVP and FlowCAM, and  
792 associated metadata and other documentation. Standards and best practices for other taxonomic  
793 datasets, such as traditional microscopy and flow cytometry are either published or underway  
794 (Neeley et al. 2023). Incorporating molecular taxonomy datasets would be the next step, as  
795 currently, these data are not easily accessible for validation or dataset-building purposes. In  
796 parallel, community accepted protocols are being developed for a whole suite of other PACE  
797 products, including hyperspectral remote sensing reflectance (Zibordi et al. 2019). As these new

798 datatypes are added to the validation pipeline, they will be included into future versions of  
799 NOMAD datasets.

800 Currently, in situ data on phytoplankton concentration and composition are still heavily biased  
801 towards some regions and/or are not directly available (Thompson and Carstensen 2022). To  
802 allow for the above-mentioned applications, it is critical that we have data that allow us to  
803 calibrate/validate satellite products, as well as to validate ESM outputs (Dierssen et al. 2020). As  
804 stated by Thompson and Carstensen (2022), this network needs to be carefully planned in order  
805 to provide the information that we will need to understand and manage climate variability and  
806 change. Several recent grassroots initiatives address the geographic biases in SeaBASS (or  
807 NOMAD) towards ocean data by sharing a large database of hyperspectral  $R_{rs}(\lambda)$  (> 7500+) along  
808 with their co-located *Chl a*, CDOM, and SPM across global freshwater and coastal (Lehman et al.  
809 2023), and coastal and open ocean ecosystems (Casey et al. 2020) but with no accompanying PCC  
810 datasets.

811 Finally, error propagation and attribution of uncertainties to PCC products are paramount. This  
812 information will determine whether an algorithm can be applied effectively and/or broadly. While  
813 uncertainty has long been a topic of discussion in the ocean color community, only recently have  
814 significant strides been made to improve uncertainty estimation and error propagation to the  
815 measured or modeled products (IOCCG 2019; Kostakis et al. 2021; McKinna et al. 2019). With  
816 more complex algorithms, such as the ones used for estimation of PCC, uncertainty associated  
817 with underlying ocean color observations (Ibrahim et al. 2022; Zhang et al. 2022) accumulates  
818 through each step in the algorithm hierarchy (Siegel et al. 2023). Ancillary data present sources  
819 of uncertainty, as well as the theoretical assumptions or empirical data used to develop the PCC

820 algorithm. As PACE has a requirement to estimate uncertainty at the level of  $R_{rs}(\lambda)$ , such  
821 cumulative uncertainty should be calculated and reported with the PCC products and used in  
822 future validation exercises in combination with contemporary validation metrics (McKinna et al.  
823 2021). Such uncertainty propagation exercises can be helpful when developing future PCC  
824 algorithms, to elucidate the interpretation of (e.g., climate driven) trends in PCC observations  
825 from space. In addition, having uncertainty as part of the harmful algal blooms (HABs) detection  
826 report is crucial for water quality managers, especially when it comes to determining the potential  
827 public health risks and implementing appropriate responses.

## 828 6.2. Data accessibility and open science

829 *Chl a*, as a heritage ocean color product, sets a high bar when it comes to data objectives and  
830 potential recognition as an Essential Ocean Variable (EOV, see Muller-Karger et al. 2018).  
831 Wilkinson et al. (2016) describe widely-accepted “FAIR” data objectives, listed below with a  
832 description of the relevant OB.DAAC practice:

- 833 ● Findable: total *Chl a* estimates from multiple satellites and sensors are indexed on the  
834 Earthdata Search website, including spatial and temporal filters.
- 835 ● Accessible: single or multiple total *Chl a* datasets may be downloaded on-demand by users  
836 or applications that authenticate with a free Earthdata account.
- 837 ● Interoperable: total *Chl a* datasets are delivered as NetCDF files, which embed metadata  
838 in a vocabulary controlled by the Climate and Forecast metadata conventions.
- 839 ● Reusable: in addition to being in the public domain, total *Chl a* datasets include metadata  
840 relevant to the ocean color research (e.g., variable units, sensor calibration parameters,  
841 and references to protocols and algorithms) that cover all aspects of the data provenance.

842 PACE ocean color products, including PCC, will be distributed via OB.DAAC, as soon as the data  
843 are available. However, it is important to understand that data will be considered “provisional”,  
844 meaning that they will not be validated (or validation is in progress) and quality may not be  
845 optimal. Assessment of the PACE data quality, i.e., validation, will be done in several steps,  
846 starting with remote sensing reflectance, followed by *Chl a* (and other products in ocean color  
847 standard suite), and ultimately PCC (when data is available).

848 PACE data products for PCC are on the path to achieve each of the FAIR principles; despite being  
849 a more complicated variable than total *Chl a* (e.g., PCC is multivariate), there is nothing  
850 structurally novel about these products. New components of the vocabulary needed for metadata  
851 about phytoplankton composition (Neeley et al., 2021) demonstrate that the ocean color  
852 research community is actively engaged in establishing standards for interoperability. The units  
853 of PCC variables are well defined, ranging from *Chl a* or carbon density to total or relative  
854 abundance. Standard methods will have to be defined so that taxa can be pooled into genera or  
855 class (or higher taxonomic levels) depending on the users and goal outcomes. One of the biggest  
856 challenges, owing to the types of models that produce L4 data products containing PCC variables,  
857 will be the complete description of data source and methodology. Variables estimated through  
858 semi-analytical algorithms are relatively easy to document, using equations or open-source  
859 software and a short list of parameters. It is more difficult to document the provenance of variable  
860 estimates that get introduced after a model-fitting procedure, such as in supervised machine  
861 learning. In this case, both the fitted, or trained, model itself and any in situ data used while  
862 training must both be FAIR (e.g., Schoening et al. 2022). OB.DAAC and SeaBASS are well suited  
863 repositories to support the data-intensive model-fitting procedures reliance on in situ data.

864 The NASA Science Mission Directorate (SMD) objectives for conducting supported missions,  
865 including PACE, through open science practices extends beyond open data. The topic of  
866 inclusivity, creating new pathways for end users to become involved in science, is also relevant to  
867 open science<sup>9</sup>. While the majority of academia and government entities have computational  
868 capacity to download and process large datasets, many of those in the broader PACE CoP may  
869 have challenges working with a large number of files in scientific data formats containing multiple  
870 parameters, like  $R_{rs}(\lambda)$ , pigments, and light attenuation, and metadata on calibration, validation,  
871 and other provenance. For this reason, the PACE Mission will develop and offer trainings,  
872 tutorials, data “recipes”, and other forms of community support to ensure that users know how  
873 to appropriately access and utilize PACE data products. Further, the PACE team will continue its  
874 work with the PACE CoP to identify further training needs and gaps, and gather feedback post-  
875 launch on continued challenges and barriers and the development of new products. The PACE  
876 team, for example, is working towards making a new type of merged “Water Quality Product”  
877 that will highlight specific products for a wide range of users. Such a merged and simplified data  
878 product, drawing from different parameters, will be adaptable and can grow as new algorithms  
879 come online. Finally, a PACE Community of Potential will also be convened; versus (and in addition  
880 to) the CoP, which is made up of more technical users. The Community of Potential will target  
881 individuals or groups (within or outside of PACE CoP) who are unfamiliar with satellite data  
882 products and PACE capabilities but may be able to leverage and benefit from PACE data products.  
883 Members of the Community of Potential may benefit from additional support on remote sensing  
884 at large, and the benefits and applications that PACE specifically could offer. For example, white

---

<sup>9</sup> <https://science.nasa.gov/open-science-overview>

885 papers with case studies may be developed so that new users can understand possible  
886 applications and uses of PACE data. In addition, certain new conferences or venues could be  
887 identified and targeted where users are less familiar with NASA remote sensing data. Other  
888 efforts to engage with new and existing users – whether for awareness raising, training, or some  
889 combination – will be considered as they are identified.

890 Steps to reduce financial barriers associated with research on PCC include provisioning of cloud-  
891 computing services with timely access to PCC data products, that should not only rely on NASA  
892 based providers. The Giovanni (10.1029/2007EO020003) and Google Earth Engine (Ugur et al  
893 2021) systems are in-browser applications coupled to cloud computing facilities that provide low-  
894 barrier entries to analysis of earth observation variables. The inclusion of new variables on  
895 phytoplankton communities in these or other comparable systems is included in the design  
896 objectives for PCC data products. Training on software and online data tools for new users will be  
897 integral to the mission.

## 898 7. Conclusion

899 In this paper we have identified the strengths and weaknesses of existing approaches and  
900 presented how PACE will address some of the remaining gaps and challenges for quantifying  
901 PCC. The knowledge gained from this mission will rely on the existence of appropriate validation  
902 products (e.g., quality, coverage, diversity of products available, error and uncertainties  
903 requirements), the use of the various approaches currently available (in situ, satellite, and  
904 model products) as well as the distribution of data products following FAIR principles including  
905 training of the community and developing user friendly data products. Improved  
906 characterization of PCC is key to understanding aquatic ecosystems, our ocean's health, and the

907 ocean's effects on global climate. From local applications, such as water quality assessments  
908 that are focused on specific phytoplankton taxa, to global applications such as the role that  
909 ocean plays in carbon sequestration, the needs for information on phytoplankton composition  
910 requires the community to work together to develop the next generation of data products. This  
911 is especially critical when it comes to improving our understanding of the impact that climate  
912 change has on the ocean and developing effective management strategies for the ocean and  
913 other aquatic resources, both today and in the future.

## 914 Acknowledgments

915 Authors highly appreciate the discussions with rest of the PACE Science and Application Team  
916 that helped conceptualize the idea of this paper. We are also grateful to PACE user community  
917 for participating in the survey. We are appreciative for comments on the earlier draft of this  
918 paper provided by Mike Behrenfeld and Zach Erickson. Authors are thankful to NASA OBB  
919 program, under Laura Lorenzoni's leadership, for funding for the PACE Science and Application  
920 Team, and Lorraine Remer and Heidi Dierssen for their leadership.

## 921 Credit author statement

922 **Ivona Cetinić:** Conceptualization, Writing - Original Draft, Writing - Review & Editing, Visualization  
923 **Cecile S. Rousseaux:** Conceptualization, Writing - Original Draft, Writing - Review & Editing,  
924 Visualization **Ian T. Carroll** Conceptualization, Writing - Original Draft, Writing - Review & Editing,  
925 Visualization **Alison P. Chase:** Conceptualization, Writing - Original Draft, Writing - Review &  
926 Editing, Visualization **Sasha J. Kramer:** Conceptualization, Writing - Original Draft, Writing -  
927 Review & Editing, Visualization **P. Jeremy Werdell** Conceptualization, Writing - Original Draft,  
928 Writing - Review & Editing **David. A. Siegel:** Conceptualization, Writing - Original Draft, **Heidi M.**

929 **Dierssen** Conceptualization, Writing - Original Draft, **Dylan Catlett**: Conceptualization, Writing -  
930 Original Draft , **Aimee Neeley**: Conceptualization, Writing - Original Draft , **Inia M. Soto Ramos**:  
931 Conceptualization, Writing - Original Draft, **Jennifer L. Wolny**: Conceptualization, Writing -  
932 Original Draft **Natasha Sadoff**: Writing - Original Draft **Erin Urquhart**: Writing - Original Draft,  
933 **Toby K. Westberry**: Writing - Review & Editing, **Dariusz Stramski**: Writing - Review & Editing,  
934 **Nima Pahlevan**: Writing - Review & Editing, **Bridget N. Seegers**: Writing - Review & Editing  
935 **Emerson Sirk**: Writing - Review & Editing, **Priscila Kienteca Lange**: Writing - Review & Editing ,  
936 **Ryan A. Vandermeulen**: Writing - Review & Editing, **Jason R. Graff**: Writing - Review & Editing,  
937 **James G. Allen**: Writing - Review & Editing, **Peter Gaube**: Writing - Review & Editing, **Lachlan I.**  
938 **W. McKinna**: Writing - Review & Editing, **S.Morgaine McKibben**: Writing - Review & Editing, **Caren**  
939 **E. Binding**: Writing - Review & Editing **Violeta Sanjuan Calzado**: Writing - Review & Editing,  
940 **Michael Sayers**: Writing - Review & Editing

941

## 942 Funding

943 I.C. was funded through PACE mission, and NSF grant 222980; C.S.R. was funded through NASA  
944 grant 80NSSC20M0208; I.T.C through PACE mission and NASA grant 80NSSC23K0045; A.P.C.  
945 through NASA grant 80NSSC20M0202 and Washington Research Foundation Postdoctoral  
946 Fellowship; S.J.K through NASA grant 80NSSC20M0226 and NASA grant 80NSSC21K0015; P.J.W  
947 through PACE mission; D.A.S. through NASA grants 80NSSC21K1750, 80NSSC20M0226, and  
948 80NSSC17K0692; H.M.D through NASA grant 80NSS20M0206; D.C. through NASA grants  
949 80NSSC21K1750, 80NSSC20M0226, and 80NSSC17K0692; A.N. through NASA/SSAI HBG Contract:  
950 80GSFC20C0044; I.M.S.R. through PACE mission; J.L.W. through 80NSSC21K0499; N.S. and E.U.

951 through NASA/SSAI HBG - PACE Mission; T.K.W. through NASA 80NSSC20M0228; D.S. through  
952 80NSSC20M0252; B.N.S. through NASA 14-SMDUNSOL14-0001 and PACE mission; N.P. through  
953 NASA grants 80NSSC20M0235 and 80NSSC21K0499; E.S. through PACE mission; P.K.L. through  
954 CNPq GOOS-BR 409666/2022-0, "Satellite analysis of shifts in phytoplankton community  
955 composition and energy flow in the new Arctic" (NOAA Joint Polar Satellite System (JPSS) Proving  
956 Ground and Risk Reduction (PGRR) program), and PACE mission; R.A.V. through PACE mission;  
957 J.R.G. through NASA grants 80NSSC20M0228 and 80NSSC17K0568; J.G.A. through NASA grant  
958 80NSSC20M0258; P.G. through 80NSSC20M0202; L.I.W.M through PACE mission; S.M.M. through  
959 NPP program; C.E.B through 80NSSC20M0235; V.S.C under PACE mission; and M.S. under NASA  
960 grant 80NSSC20M0223.

961

## 962 References

- 963 Aguirre-Gómez, R., Boxall, S., & Weeks, A. (2001). Detecting photosynthetic algal pigments in natural  
964 populations using a high-spectral-resolution spectroradiometer. *International Journal of Remote Sensing*,  
965 22, 2867-2884
- 966 Aitchison, J. (1982). The statistical analysis of compositional data. *Journal of the Royal Statistical Society:*  
967 *Series B (Methodological)*, 44, 139-160
- 968 Alvain, S., Moulin, C., Dandonneau, Y., & Bréon, F.-M. (2005). Remote sensing of phytoplankton groups in  
969 case 1 waters from global SeaWiFS imagery. *Deep Sea Research Part I: Oceanographic Research Papers*,  
970 52, 1989-2004
- 971 Alvain, S., Moulin, C., Dandonneau, Y., & Loisel, H. (2008). Seasonal distribution and succession of  
972 dominant phytoplankton groups in the global ocean: A satellite view. *Global Biogeochemical Cycles*, 22
- 973 Anderson, C.R., Siegel, D.A., Kudela, R.M., & Brzezinski, M.A. (2009). Empirical models of toxigenic  
974 Pseudo-nitzschia blooms: potential use as a remote detection tool in the Santa Barbara Channel. *Harmful*  
975 *Algae*, 8, 478-492
- 976 Anderson, C.R., Berdalet, E., Kudela, R.M., Cusack, C.K., Silke, J., O'Rourke, E., Dugan, D., McCammon, M.,  
977 Newton, J.A., Moore, S.K. & Paige, K., (2019). Scaling up from regional case studies to a global harmful  
978 algal bloom observing system. *Frontiers in Marine Science*, 9
- 979 Anderson, S.I., Barton, A.D., Clayton, S., Dutkiewicz, S., & Rynearson, T.A. (2021). Marine phytoplankton  
980 functional types exhibit diverse responses to thermal change. *Nature Communications*, 12, 6413
- 981 Aurin, D., Mannino, A., & Franz, B. (2013). Spatially resolving ocean color and sediment dispersion in  
982 river plumes, coastal systems, and continental shelf waters. *Remote Sensing of Environment*, 137, 212-  
983 225

984 Behrenfeld, M.J., O'Malley, R.T., Siegel, D.A., McClain, C.R., Sarmiento, J.L., G.C., F., Milligan, A.J.,  
985 Falkowski, P.G., Letelier, R.M., & Boss, E.S. (2006). Climate-driven trends in contemporary ocean  
986 productivity. *Nature*, 444, 752-755

987 Beardall, J., Allen, D., Bragg, J., Finkel, Z.V., Flynn, K.J., Quigg, A., Rees, T.A.V., Richardson, A., & Raven,  
988 J.A. (2009). Allometry and stoichiometry of unicellular, colonial and multicellular phytoplankton. *New  
989 Phytologist*, 181, 295-309

990 Ben Mustapha, Z., Alvain, S., Jamet, C., Loisel, H., & Dessailly, D. (2014). Automatic classification of  
991 water-leaving radiance anomalies from global SeaWiFS imagery: Application to the detection of  
992 phytoplankton groups in open ocean waters. *Remote Sensing of Environment*, 146, 97-112

993 Bernard, S., Kudela, R. M., Robertson Lain, L., & Pitcher, G. (2021). Observation of harmful algal blooms  
994 with ocean colour radiometry. International Ocean-Colour Coordinating Group (IOCCG) Report Series,  
995 No. 20, Dartmouth, Canada. <http://dx.doi.org/10.25607/OBP-1042>

996 Bopp, L., Aumont, O., Cadule, P.,  
997 Alvain, S., & Gehlen, M. (2005). Response of diatoms distribution to global warming and potential  
998 implications: A global model study. *Geophysical Research Letters*, 32, n/a-n/a

999 Boss, E., M.S. Twardowski, & Herring, S. (2001). Shape of particulate beam attenuation spectrum and its  
inversion to obtain the shape of the particle size distribution. *Applied Optics*, 40, 4885-4893

1000 Bracher, A., Bouman, H.A., Brewin, R.J.W., Bricaud, A., Brotas, V., Ciotti, A.M., Clementson, L., Devred, E.,  
1001 Di Cicco, A., Dutkiewicz, S., Hardman-Mountford, N.J., Hickman, A.E., Hieronymi, M., Hirata, T., Losa, S.N.,  
1002 Mouw, C.B., Organelli, E., Raitsos, D.E., Uitz, J., Vogt, M., & Wolanin, A. (2017). Obtaining Phytoplankton  
1003 Diversity from Ocean Color: A Scientific Roadmap for Future Development. *Frontiers in Marine Science*, 4

1004 Bracher, A., Brewin, R.J.W., Ciotti, A.M., Clementson, L.A., Hirata, T., Kostadinov, T.S., Mouw, C.B., &  
1005 Organelli, E. (2022). Chapter 7 - Applications of satellite remote sensing technology to the analysis of  
1006 phytoplankton community structure on large scales. In L.A. Clementson, R.S. Eriksen, & A. Willis (Eds.),  
1007 *Advances in Phytoplankton Ecology* (pp. 217-244): Elsevier

1008 Bracher, A., Taylor, M.H., Taylor, B., Dinter, T., Röttgers, R., & Steinmetz, F. (2015). Using empirical  
1009 orthogonal functions derived from remote-sensing reflectance for the prediction of phytoplankton  
1010 pigment concentrations. *Ocean Science*, 11, 139-158

1011 Bracher, A., Vountas, M., Dinter, T., Burrows, J., Röttgers, R., & Peeken, I. (2009). Quantitative  
1012 observation of cyanobacteria and diatoms from space using PhytoDOAS on SCIAMACHY data.  
1013 *Biogeosciences*, 6, 751-764

1014 Bradley, I.M., Pinto, A.J., Guest, J.S., & Voordouw, G. (2016). Design and Evaluation of Illumina MiSeq-  
1015 Compatible, 18S rRNA Gene-Specific Primers for Improved Characterization of Mixed Phototrophic  
1016 Communities. *Applied and Environmental Microbiology*, 82, 5878-5891

1017 Brewin, R.J.W., Ciavatta, S., Sathyendranath, S., Jackson, T., Tilstone, G., Curran, K., Airs, R.L., Cummings,  
1018 D., Brotas, V., Organelli, E., Dall'Olmo, G., & Raitsos, D.E. (2017). Uncertainty in Ocean-Color Estimates of  
1019 Chlorophyll for Phytoplankton Groups. *Frontiers in Marine Science*, 4

1020 Brewin, R.J., Hardman-Mountford, N.J., Lavender, S.J., Raitsos, D.E., Hirata, T., Uitz, J., Devred, E.,  
1021 Bricaud, A., Ciotti, A., & Gentili, B. (2011a). An intercomparison of bio-optical techniques for detecting  
1022 dominant phytoplankton size class from satellite remote sensing. *Remote Sensing of Environment*, 115,  
1023 325-339

1024 Brewin, R.J., Sathyendranath, S., Hirata, T., Lavender, S.J., Barciela, R.M., & Hardman-Mountford, N.J.  
1025 (2010). A three-component model of phytoplankton size class for the Atlantic Ocean. *Ecological  
1026 Modelling*, 221, 1472-1483

1027 Brewin, R.J., Sathyendranath, S., Jackson, T., Barlow, R., Brotas, V., Airs, R., & Lamont, T. (2015).  
1028 Influence of light in the mixed-layer on the parameters of a three-component model of phytoplankton  
1029 size class. *Remote Sensing of Environment*, 168, 437-450

1030 Brewin, R.J.W., Devred, E., Sathyendranath, S., Lavender, S.J., & Hardman-Mountford, N.J. (2011b).  
1031 Model of phytoplankton absorption based on three size classes. *Applied Optics*, 50, 4535-4549

1032 Bricaud, A., Ciotti, A.M., & Gentili, B. (2012). Spatial-temporal variations in phytoplankton size and  
1033 colored detrital matter absorption at global and regional scales, as derived from twelve years of SeaWiFS  
1034 data (1998&#8211;2009). *Global Biogeochemical Cycles*, *26*, GB1010

1035 Bricaud, A., Mejjia, C., Blondeau-Patissier, D., Claustre, H., Crepon, M., & Thiria, S. (2007). Retrieval of  
1036 pigment concentrations and size structure of algal populations from their absorption spectra using  
1037 multilayered perceptrons. *Applied Optics*, *46*, 1251-1260

1038 Briggs, N., Guðmundsson, K., Cetinić, I., D'Asaro, E., Rehm, E., Lee, C., & Perry, M.J. (2018). A multi-  
1039 method autonomous assessment of primary productivity and export efficiency in the springtime North  
1040 Atlantic. *Biogeosciences*, *15*, 4515-4532

1041 Brown, C.W., & Yoder, J.A. (1994). Coccolithophorid blooms in the global ocean. *Journal of Geophysical  
1042 Research: Oceans*, *99*, 7467-7482

1043 Cael, B., Chase, A., & Boss, E. (2020). Information content of absorption spectra and implications for  
1044 ocean color inversion. *Applied Optics*, *59*, 3971-3984

1045 Cael, B.B., Begouen Demeaux, C., Henson, S., Stock, C.A., Taboada, F.G., John, J.G., & Barton, A.D.  
1046 (2022a). Marine Ecosystem Changepoints Spread Under Ocean Warming in an Earth System Model.  
1047 *Journal of Geophysical Research: Biogeosciences*, *127*, e2021JG006571

1048 Cael, B.B., Bisson, K., Boss, E., Dutkiewicz, S., & Henson, S. (2022c). Global climate change trends  
1049 detected in indicators of ocean ecology. *EarthArXiv*

1050 Cael, B. B., Bisson, K.M., Boss, E. S. & Erickson, Z. (2022b). Extracting information from ocean color.  
1051 *Authorea*.

1052 Calvo-Díaz, A., & Morán, X.A.G. (2006). Seasonal dynamics of picoplankton in shelf waters of the  
1053 southern Bay of Biscay. *Aquatic Microbial Ecology*, *42*, 159-174

1054 Caracappa, J. C., Beet, A., Gaichas, S., Gamble, R. J., Hyde, K. J., Large, S. I., ... & Saba, V. S. (2022). A  
1055 northeast United States Atlantis marine ecosystem model with ocean reanalysis and ocean color forcing.  
1056 *Ecological Modelling*, *471*, 110038.

1057 Castagna, A., Dierssen, H., Organelli, E., Bogorad, M., Mortelmans, J., Vyverman, W., & Sabbe, K. (2021).  
1058 Optical Detection of Harmful Algal Blooms in the Belgian Coastal Zone: A Cautionary Tale of Chlorophyll  
1059 c3. *Frontiers in Marine Science*, *8*

1060 Casey, J. R., Aucan, J. P., Goldberg, S. R., & Lomas, M. W. (2013). Changes in partitioning of carbon  
1061 amongst photosynthetic pico-and nano-plankton groups in the Sargasso Sea in response to changes in  
1062 the North Atlantic Oscillation. *Deep Sea Research Part II: Topical Studies in Oceanography*, *93*, 58-70.

1063 Casey, K. A., Rousseaux, C. S., Gregg, W. W., Boss, E., Chase, A. P., Craig, S. E., ... & Maritorena, S. (2020).  
1064 A global compilation of in situ aquatic high spectral resolution inherent and apparent optical property  
1065 data for remote sensing applications. *Earth system science data*, *12*, 1123-1139

1066 Catlett, D., Matson, P.G., Carlson, C.A., Wilbanks, E.G., Siegel, D.A., & Iglesias-Rodriguez, M.D. (2020).  
1067 Evaluation of accuracy and precision in an amplicon sequencing workflow for marine protist  
1068 communities. *Limnology and Oceanography: Methods*, *18*, 20-40

1069 Catlett, D., Siegel, D.A., Matson, P.G., Wear, E.K., Carlson, C.A., Lankiewicz, T.S., & Iglesias-Rodriguez,  
1070 M.D. (2022). Integrating phytoplankton pigment and DNA meta-barcoding observations to determine  
1071 phytoplankton composition in the coastal ocean. *In revision at Limnology and Oceanography*

1072 Catlett, D., Siegel, D.A., Simons, R.D., Guillocheau, N., Henderikx-Freitas, F., & Thomas, C.S. (2021).  
1073 Diagnosing seasonal to multi-decadal phytoplankton group dynamics in a highly productive coastal  
1074 ecosystem. *Progress in Oceanography*, *197*, 102637

1075 Catlett, D.S., & Siegel, D.A. (2018). Phytoplankton Pigment Communities Can be Modeled Using Unique  
1076 Relationships With Spectral Absorption Signatures in a Dynamic Coastal Environment. *Journal of  
1077 Geophysical Research: Oceans*, *123*, 246-264

1078 Chase, A., Boss, E., Zaneveld, R., Bricaud, A., Claustre, H., Ras, J., Dall'Olmo, G., & Westberry, T.K. (2013).  
1079 Decomposition of in situ particulate absorption spectra. *Methods in Oceanography*, *7*, 110-124

1080 Chase, A.P., Boss, E., Cetinić, I., & Slade, W. (2017). Estimation of Phytoplankton Accessory Pigments  
1081 From Hyperspectral Reflectance Spectra: Toward a Global Algorithm. *Journal of Geophysical Research:*  
1082 *Oceans*, 122, 9725-9743

1083 Chase, A.P., Boss, E.S., Haëntjens, N., Culhane, E., Roesler, C., & Karp-Boss, L. (2022). Plankton Imagery  
1084 Data Inform Satellite-Based Estimates of Diatom Carbon. *Geophysical Research Letters*, 49,  
1085 e2022GL098076

1086 Chase, A.P., Kramer, S.J., Haëntjens, N., Boss, E.S., Karp-Boss, L., Edmondson, M., & Graff, J.R. (2020).  
1087 Evaluation of diagnostic pigments to estimate phytoplankton size classes. *Limnology and Oceanography:*  
1088 *Methods*, 18, 570-584

1089 Chowdhary, J., Zhai, P.-W., Boss, E., Dierssen, H., Frouin, R., Ibrahim, A., Lee, Z., Remer, L.A., Twardowski,  
1090 M., Xu, F., Zhang, X., Ottaviani, M., Espinosa, W.R., & Ramon, D. (2019). Modeling Atmosphere-Ocean  
1091 Radiative Transfer: A PACE Mission Perspective. *Frontiers in Earth Science*, 7

1092 Ciavatta, S., Brewin, R., Skakala, J., Polimene, L., de Mora, L., Artioli, Y., & Allen, J.I. (2018). Assimilation of  
1093 ocean-color plankton functional types to improve marine ecosystem simulations. *Journal of Geophysical*  
1094 *Research: Oceans*, 123, 834-854

1095 Ciotti, A.M., & Bricaud, A. (2006). Retrievals of a size parameter for phytoplankton and spectral light  
1096 absorption by colored detrital matter from water-leaving radiances at SeaWiFS channels in a continental  
1097 shelf region off Brazil. *Limnology and Oceanography: Methods*, 4, 237-253

1098 Claustre, H., Bricaud, A., Babin, M., Bruyant, F., Guillou, L., Le Gall, F., Marie, D., & Partensky, F. (2002).  
1099 Diel variations in Prochlorococcus optical properties. *Limnology and Oceanography*, 47, 1637-1647

1100 Clayton, S., Gibala-Smith, L., Mogatas, K., Flores-Vargas, C., Marciniak, K., Wigginton, M., & Mulholland,  
1101 M.R. (2022). Imaging Technologies Build Capacity and Accessibility in Phytoplankton Species  
1102 Identification Expertise for Research and Monitoring: Lessons Learned During the COVID-19 Pandemic.  
1103 *Frontiers in Microbiology*, 13, 823109

1104 Concha, J., Mannino, A., Franz, B., & Kim, W. (2019). Uncertainties in the Geostationary Ocean Color  
1105 Imager (GOCI) Remote Sensing Reflectance for Assessing Diurnal Variability of Biogeochemical Processes.  
1106 *Remote Sensing*, 11, 295

1107 Craig, S.E., Lohrenz, S.E., Lee, Z.P., Mahoney, K.L., Kirkpatrick, G.J., Schofield, O.M., & Steward, R.G.  
1108 (2006). Use of hyperspectral remote sensing reflectance for detection and assessment of the harmful  
1109 alga, *Karenia brevis*. *Applied Optics*, 45, 5414-5425

1110 Cram, J. A., Weber, T., Leung, S. W., McDonnell, A. M., Liang, J. H., & Deutsch, C. (2018). The role of  
1111 particle size, ballast, temperature, and oxygen in the sinking flux to the deep sea. *Global Biogeochemical*  
1112 *Cycles*, 32, 858-876

1113 de Vargas, C., Audic, S., Henry, N., Decelle, J., Mahé, F., Logares, R., Lara, E., Berney, C., Le Bescot, N.,  
1114 Probert, I., ...& Karsenti, E. (2015). Eukaryotic plankton diversity in the sunlit ocean. *Science*, 348,  
1115 1261605

1116 Defoin-Platel, M., & Chami, M. (2007). How ambiguous is the inverse problem of ocean color in coastal  
1117 waters? *Journal of Geophysical Research: Oceans*, 112

1118 Devred, E., Sathyendranath, S., Stuart, V., Maass, H., Ulloa, O., & Platt, T. (2006). A two-component  
1119 model of phytoplankton absorption in the open ocean: Theory and applications. *Journal of Geophysical*  
1120 *Research*, 111

1121 Devred, E., Sathyendranath, S., Stuart, V., & Platt, T. (2011). A three component classification of  
1122 phytoplankton absorption spectra: Application to ocean-color data. *Remote Sensing of Environment*, 115,  
1123 2255-2266

1124 Di Cicco, A., Sammartino, M., Marullo, S., & Santoleri, R. (2017). Regional Empirical Algorithms for an  
1125 Improved Identification of Phytoplankton Functional Types and Size Classes in the Mediterranean Sea  
1126 Using Satellite Data. *Frontiers in Marine Science*, 4

1127 Dierssen, H., Bracher, A., Brando, V., Loisel, H., & Ruddick, K. (2020). Data needs for hyperspectral  
1128 detection of algal diversity across the globe. *Oceanography*, 33, 74-79

1129 Dierssen, H., McManus, G.B., Chlus, A., Qiu, D., Gao, B.-C., & Lin, S. (2015). Space station image captures  
1130 a red tide ciliate bloom at high spectral and spatial resolution. *Proceedings of the National Academy of  
1131 Sciences*, 112, 14783-14787

1132 Dinauer, A., Laufkötter, C., Doney, S.C., & Joos, F. (2022). What Controls the Large-Scale Efficiency of  
1133 Carbon Transfer Through the Ocean's Mesopelagic Zone? Insights From a New, Mechanistic Model  
1134 (MSPACMAM). *Global Biogeochemical Cycles*, 36, e2021GB007131

1135 Dupouy, C., Benielli-Gary, D., Neveux, J., Dandonneau, Y., & Westberry, T.K. (2011). An algorithm for  
1136 detecting Trichodesmium surface blooms in the South Western Tropical Pacific. *Biogeosciences*, 8, 3631-  
1137 3647

1138 Durden, J.M., Luo, J.Y., Alexander, H., Flanagan, A.M., & Grossmann, L. (2017). Integrating “Big Data” into  
1139 Aquatic Ecology: Challenges and Opportunities. *Limnology and Oceanography Bulletin*, 26, 101-108

1140 Dutkiewicz, S., Cermeno, P., Jahn, O., Follows, M.J., Hickman, A.E., Taniguchi, D.A.A., & Ward, B.A.  
1141 (2020). Dimensions of marine phytoplankton diversity. *Biogeosciences*, 17, 609-634

1142 Dutkiewicz, S., Scott, J.R., & Follows, M.J. (2013). Winners and losers: Ecological and biogeochemical  
1143 changes in a warming ocean. *Global Biogeochemical Cycles*, 27, 463-477

1144 Eayrs, C., Li, X., Raphael, M.N., & Holland, D.M. (2021). Rapid decline in Antarctic sea ice in recent years  
1145 hints at future change. *Nature Geoscience*, 14, 460-464

1146 Elder, L., & Elbrächter, M. (2010). The Utermöhl method for quantitative phytoplankton analysis. In B.  
1147 Karlson, C. Cusack, & E. Bresnan (Eds.), *Microscopic and molecular methods for quantitative  
1148 phytoplankton analysis*. PARIS: UNESCO

1149 Erickson, Z. K., Frankenberg, C., Thompson, D. R., Thompson, A. F., & Gierach, M. (2019). Remote sensing  
1150 of chlorophyll fluorescence in the ocean using imaging spectrometry: toward a vertical profile of  
1151 fluorescence. *Geophysical Research Letters*, 46, 1571-1579.

1152 Fisher, J.L., Peterson, W.T., & Rykaczewski, R.R. (2015). The impact of El Niño events on the pelagic food  
1153 chain in the northern California Current. *Global Change Biology*, 21, 4401-4414

1154 Flexas, M.M., Thompson, A.F., Schodlok, M.P., Zhang, H., & Speer, K. (2022). Antarctic Peninsula warming  
1155 triggers enhanced basal melt rates throughout West Antarctica. *Science Advances*, 8, eabj9134

1156 Forget, M.-H.I.n., Carignan, R., & Hudon, C. (2009). Influence of diel cycles of respiration, chlorophyll, and  
1157 photosynthetic parameters on the summer metabolic balance of temperate lakes and rivers. *Canadian  
1158 Journal of Fisheries & Aquatic Sciences*, 66, 1048-1058

1159 Franz, B.A., Cetinic, I., Scott, J.P., Siegel, A., & Westberry, T.K. (2021). Global ocean phytoplankton [in  
1160 “State of the Climate in 2020”]. *Bulletin of the American Meteorological Society*, 102, S179 - S193

1161 Frieder, C.A., Yan, C., Chamecki, M., Dauhajre, D., McWilliams, J.C., Infante, J., McPherson, M.L., Kudela,  
1162 R.M., Kessouri, F., Sutula, M., Arzeno-Soltero, I.B., & Davis, K.A. (2022). A Macroalgal Cultivation  
1163 Modeling System (MACMODS): Evaluating the Role of Physical-Biological Coupling on Nutrients and Farm  
1164 Yield. *Frontiers in Marine Science*, 9

1165 Frouin, R.J., Franz, B.A., Ibrahim, A., Knobelspiesse, K., Ahmad, Z., Cairns, B., Chowdhary, J., Dierssen,  
1166 H.M., Tan, J., Dubovik, O., Huang, X., Davis, A.B., Kalashnikova, O., Thompson, D.R., Remer, L.A., Boss, E.,  
1167 Coddington, O., Deschamps, P.-Y., Gao, B.-C., Gross, L., Hasekamp, O., Omar, A., Pelletier, B., Ramon, D.,  
1168 Steinmetz, F., & Zhai, P.-W. (2019). Atmospheric Correction of Satellite Ocean-Color Imagery During the  
1169 PACE Era. *Frontiers in Earth Science*, 7

1170 Fujiwara, A., Hirawake, T., Suzuki, K., & Saitoh, S.-I. (2011). Remote sensing of size structure of  
1171 phytoplankton communities using optical properties of the Chukchi and Bering Sea shelf region.  
1172 *Biogeosciences*, 8, 3567

1173 Fuss, S., Canadell, J.G., Peters, G.P., Tavoni, M., Andrew, R.M., Ciais, P., Jackson, R.B., Jones, C.D.,  
 1174 Kraxner, F., Nakićenovic, N., Le Quéré, C., Raupach, M.R., Sharifi, A., Smith, P., & Yamagata, Y. (2014).  
 1175 Betting on negative emissions. *Nature Climate Change*, 4, 850-853  
 1176 Garver, S.A., Siegel, D.A., & Mitchell, B.G. (1994). Variability in near-surface particulate absorption  
 1177 spectra: What can a satellite ocean color imager see? *Limnology and Oceanography*, 39, 1349-1367  
 1178 GESAMP (2019). Guidelines for the monitoring and assessment of plastic litter in the ocean-GESAMP  
 1179 reports and studies no. 99. In P. Kershaw, A. Turra, & F. Galgani (Eds.), *GESAMP Reports and Studies* (p.  
 1180 130): IMO/FAO/UNESCO-IOC/UNIDO/WMO/IAEA/UN/UNEP/UNDP/ISA Joint Group of Experts on the  
 1181 Scientific Aspects of Marine Environmental Protection  
 1182 Gernez, P., Reynolds, R. A., & Stramski, D. (2014). Within-day variability of particulate organic carbon and  
 1183 remote-sensing reflectance during a bloom of *Phaeocystis antarctica* in the Ross Sea, Antarctica.  
 1184 *International Journal of Remote Sensing*, 35, 454-477.  
 1185 Gitelson, A.A., Gao, B.-C., Li, R.-R., Berdnikov, S., & Sapygin, V. (2011). Estimation of chlorophyll-a  
 1186 concentration in productive turbid waters using a Hyperspectral Imager for the Coastal Ocean—the Azov  
 1187 Sea case study. *Environmental Research Letters*, 6, 024023  
 1188 Gittings, J.A., Brewin, R.J., Raitsos, D.E., Kheireddine, M., Ouhssain, M., Jones, B.H., & Hoteit, I. (2019).  
 1189 Remotely sensing phytoplankton size structure in the Red Sea. *Remote Sensing of Environment*, 234,  
 1190 111387  
 1191 Gloor, G.B., Macklaim, J.M., Pawlowsky-Glahn, V., & Egozcue, J.J. (2017). Microbiome Datasets Are  
 1192 Compositional: And This Is Not Optional. *Frontiers in Microbiology*, 8  
 1193 Godhe, A., Asplund, M.E., Härnström, K., Saravanan, V., Tyagi, A., & Karunasagar, I. (2008). Quantification  
 1194 of diatom and dinoflagellate biomasses in coastal marine seawater samples by real-time PCR. *Applied  
 1195 and Environmental Microbiology*, 74, 7174-7182  
 1196 Godhe, A., Cusack, C., Pedersen, J., Andersen, P., Anderson, D.M., Bresnan, E., Cembella, A., Dahl, E.,  
 1197 Diercks, S., Elbrächter, M., Edler, L., Galluzzi, L., Gescher, C., Gladstone, M., Karlson, B., Kulis, D.,  
 1198 LeGresley, M., Lindahl, O., Marin, R., McDermott, G., Medlin, L.K., Naustvoll, L.-J., Penna, A., & Töbe, K.  
 1199 (2007). Intercalibration of classical and molecular techniques for identification of *Alexandrium fundyense*  
 1200 (Dinophyceae) and estimation of cell densities. *Harmful Algae*, 6, 56-72  
 1201 Gong, W., & Marchetti, A. (2019). Estimation of 18S Gene Copy Number in Marine Eukaryotic Plankton  
 1202 Using a Next-Generation Sequencing Approach. *Frontiers in Marine Science*, 6  
 1203 Gordon, H. R., & McCluney, W. R. (1975). Estimation of the depth of sunlight penetration in the sea for  
 1204 remote sensing. *Applied optics*, 14, 413-416  
 1205 Gowen, R.J. (1994). Managing eutrophication associated with aquaculture development. *Journal of  
 1206 Applied Ichthyology*, 10, 242-257  
 1207 Graff, J. R., Milligan, A. J., & Behrenfeld, M. J., (2012). The measurement of phytoplankton biomass using  
 1208 flow-cytometric sorting and elemental analysis of carbon. *Limnology and Oceanography Methods*, 10  
 1209 Gregg, W.W., & Casey, N.W. (2007). Modeling coccolithophores in the global oceans. *Deep Sea Research  
 1210 Part II: Topical Studies in Oceanography*, 54, 447-477  
 1211 Gregg, W.W., & Rousseaux, C.S. (2014). Decadal trends in global pelagic ocean chlorophyll: A new  
 1212 assessment integrating multiple satellites, in situ data, and models. *Journal of Geophysical Research:  
 1213 Oceans*, 119, 5921-5933  
 1214 Gregg, W.W., Rousseaux, C.S., & Franz, B.A. (2017). Global trends in ocean phytoplankton: a new  
 1215 assessment using revised ocean colour data. *Remote Sensing Letters*, 8, 1102-1111  
 1216 Guidi, L., Legendre, L., Reygondeau, G., Uitz, J., Stemmann, L., & Henson, S.A. (2015). A new look at  
 1217 ocean carbon remineralization for estimating deepwater sequestration. *Global Biogeochemical Cycles*,  
 1218 29, 1044-1059

1219 Ha, S.-Y., Min, J.-O., Joo, H., Kim, M.-S., Kang, S.-H., & Shin, K.-H. (2018). Synthesis of mycosporine-like  
1220 amino acids by a size-fractionated marine phytoplankton community of the arctic beaufort sea. *Journal*  
1221 *of Photochemistry and Photobiology B: Biology*, *188*, 87-94

1222 Haas, L.W., & Marshall, H.G. (1989). A comparison of the utermohl and epifluorescent microscopic  
1223 techniques for quantifying natural picophytoplankton

1224 Haëntjens, N., Boss, E.S., Graff, J.R., Chase, A.P., & Karp-Boss, L. (2022). Phytoplankton size distributions  
1225 in the western North Atlantic and their seasonal variability. *Limnology and Oceanography*, *67*, 1865-1878

1226 Harvey, H.W. (1934). Measurement of Phytoplankton Population. *Journal of the Marine Biological*  
1227 *Association of the United Kingdom*, *19*, 761-773

1228 Hasekamp, O.P., Fu, G., Rusli, S.P., Wu, L., Di Noia, A., Brugh, J.a.d., Landgraf, J., Martijn Smit, J., Rietjens,  
1229 J., & van Amerongen, A. (2019). Aerosol measurements by SPEXone on the NASA PACE mission: expected  
1230 retrieval capabilities. *Journal of Quantitative Spectroscopy and Radiative Transfer*, *227*, 170-184

1231 Havskum, H., Schlüter, L., Scharek, R., Berdalet, E., & Jacquet, S. (2004). Routine quantification of  
1232 phytoplankton groups—microscopy or pigment analyses? *Marine Ecology Progress Series*, *273*, 31-42

1233 Henderikx Freitas, F., & Dierssen, H.M. (2019). Evaluating the seasonal and decadal performance of red  
1234 band difference algorithms for chlorophyll in an optically complex estuary with winter and summer  
1235 blooms. *Remote Sensing of Environment*, *231*, 111228

1236 Henderikx Freitas, F., Dugenne, M., Ribalet, F., Hynes, A., Barone, B., Karl, D.M., & White, A.E. (2020).  
1237 Diel variability of bulk optical properties associated with the growth and division of small phytoplankton  
1238 in the North Pacific Subtropical Gyre. *Applied Optics*, *59*, 6702-6716

1239 Henriksen, P., Riemann, B., Kaas, H., Sørensen, H.M., & Sørensen, H.L. (2002). Effects of nutrient-  
1240 limitation and irradiance on marine phytoplankton pigments. *Journal of Plankton Research*, *24*, 835-858

1241 Henson, S.A., Laufkötter, C., Leung, S., Giering, S.L.C., Palevsky, H.I., & Cavan, E.L. (2022). Uncertain  
1242 response of ocean biological carbon export in a changing world. *Nature Geoscience*, *15*, 248-254

1243 Henson, S.A., Sarmiento, J.L., Dunne, J.P., Bopp, L., Lima, I., Doney, S.C., John, J., & Beaulieu, C. (2010).  
1244 Detection of anthropogenic climate change in satellite records of ocean chlorophyll and productivity.  
1245 *Biogeosciences*, *7*, 621-640

1246 Hirata, T., Aiken, J., Hardman-Mountford, N., Smyth, T., & Barlow, R. (2008). An absorption model to  
1247 determine phytoplankton size classes from satellite ocean colour. *Remote Sensing of Environment*, *112*,  
1248 3153-3159

1249 Hirata, T., Hardman-Mountford, N., Brewin, R., Aiken, J., Barlow, R., Suzuki, K., Isada, T., Howell, E.,  
1250 Hashioka, T., & Noguchi-Aita, M. (2011). Synoptic relationships between surface Chlorophyll-a and  
1251 diagnostic pigments specific to phytoplankton functional types. *Biogeosciences*, *8*, 311

1252 Hoepffner, N., & Sathyendranath, S. (1991). Effect of pigment composition on absorption properties of  
1253 phytoplankton. *Mar. Ecol. Prog. Ser.*, *73*, 1-23

1254 Hoepffner, N., & Sathyendranath, S. (1993). Determination of the Major Groups of Phytoplankton  
1255 Pigments from the Absorption-Spectra of Total Particulate Matter. *Journal of Geophysical Research-*  
1256 *Oceans*, *98*, 22789-22803

1257 Hooker, S.B., Clementson, L., Thomas, C.S., Schlüter, L., Allerup, M., Ras, J., Claustre, H., Normandeau, C.,  
1258 Cullen, J.J., Kienast, M., Kozłowski, W., Vernet, M., Chakraborty, S., Lohrenz, S.E., Tuel, M., Redalje, D.,  
1259 Cartaxana, P., Mendes, C.R., Brotas, V., Prabhu Matondkar, S.G., Parab, S.G., Neeley, A., & Egeland, E.S.  
1260 (2012). The Fifth SeaWiFS HPLC Analysis Round-Robin Experiment (SeaHARRE-5). In *NASA Technical*  
1261 *Reports* (pp. 1-108). Greenbelt, Maryland: NASA Goddard Space Flight Center

1262 Hu, C., Cannizzaro, J., Carder, K.L., Muller-Karger, F.E., & Hardy, R. (2010). Remote detection of  
1263 Trichodesmium blooms in optically complex coastal waters: Examples with MODIS full-spectral data.  
1264 *Remote Sensing of Environment*, *114*, 2048-2058

1265 Hunter-Cevera, K.R., Hamilton, B.R., Neubert, M.G., & Sosik, H.M. (2021). Seasonal environmental  
1266 variability drives microdiversity within a coastal *Synechococcus* population. *Environmental Microbiology*,  
1267 23, 4689-4705

1268 Ibrahim, A., Franz, B., Ahmad, Z., Healy, R., Knobelspiesse, K., Gao, B.-C., Proctor, C., & Zhai, P.-W. (2018).  
1269 Atmospheric correction for hyperspectral ocean color retrieval with application to the Hyperspectral  
1270 Imager for the Coastal Ocean (HICO). *Remote Sensing of Environment*, 204, 60-75

1271 Ibrahim, A., Franz, B.A., Sayer, A.M., Knobelspiesse, K., Zhang, M., Bailey, S.W., McKinna, L.I.W., Gao, M.,  
1272 & Werdell, P.J. (2022). Optimal estimation framework for ocean color atmospheric correction and pixel-  
1273 level uncertainty quantification. *Applied Optics*, 61, 6453-6475

1274 IOCCG (2014). *Phytoplankton Functional Types from Space*. Dartmouth, Canada: IOCCG

1275 IOCCG (2019). *Uncertainties in Ocean Colour Remote Sensing*. Dartmouth, Canada: IOCCG

1276 IOCCG (2020). *Synergy between Ocean Colour and Biogeochemical/Ecosystem Models*. Dartmouth,  
1277 Canada: IOCCG

1278 IPCC (2019). Special Report on the Ocean and Cryosphere in a Changing Climate. In H.-O. Pörtner, D.C.  
1279 Roberts, V. Masson-Delmotte, P. Zhai, M. Tignor, E. Poloczanska, K. Mintenbeck, A. Alegría, M. Nicolai, A.  
1280 Okem, J. Petzold, B. Rama, & N.M. Weyer (Eds.). Cambridge, United Kingdom and New York, NY, USA

1281 IPCC (2021). Climate Change 2021: The Physical Science Basis. Contribution of Working Group I to the  
1282 Sixth Assessment Report of the Intergovernmental Panel on Climate Change. In V. Masson-Delmotte, P.  
1283 Zhai, A. Pirani, S.L. Connors, C. Péan, S. Berger, N. Caud, Y. Chen, L. Goldfarb, M.I. Gomis, M. Huang, K.  
1284 Leitzell, E. Lonnoy, J.B.R. Matthews, T.K. Maycock, T. Waterfield, O. Yelekçi, R. Yu, & B. Zhou (Eds.).  
1285 Cambridge, United Kingdom and New York, NY, USA: Cambridge University Press

1286 Isada, T., Hirawake, T., Kobayashi, T., Nosaka, Y., Natsuike, M., Imai, I., Suzuki, K., & Saitoh, S.-I. (2015).  
1287 Hyperspectral optical discrimination of phytoplankton community structure in Funka Bay and its  
1288 implications for ocean color remote sensing of diatoms. *Remote Sensing of Environment*, 159, 134-151

1289 Jamet, C., Ibrahim, A., Ahmad, Z., Angelini, F., Babin, M., Behrenfeld, M.J., Boss, E., Cairns, B., Churnside,  
1290 J., Chowdhary, J., Davis, A.B., Dionisi, D., Duforêt-Gaurier, L., Franz, B., Frouin, R., Gao, M., Gray, D.,  
1291 Hasekamp, O., He, X., Hostetler, C., Kalashnikova, O.V., Knobelspiesse, K., Lacour, L., Loisel, H., Martins,  
1292 V., Rehm, E., Remer, L., Sanhaj, I., Stamnes, K., Stamnes, S., Victori, S., Werdell, J., & Zhai, P.-W. (2019).  
1293 Going Beyond Standard Ocean Color Observations: Lidar and Polarimetry. *Frontiers in Marine Science*, 6

1294 Jeffrey, S., MacTavish, H., Dunlap, W., Vesk, M., & Groenewoud, K. (1999). Occurrence of UVA-and UVB-  
1295 absorbing compounds in 152 species (206 strains) of marine microalgae. *Marine Ecology Progress Series*,  
1296 189, 35-51

1297 Jeffrey, S.W., Wright, S.W., & Zapata, M. (2011). Microalgal classes and their signature pigments. In S.  
1298 Roy, C.A. Llewellyn, E.S. Egeland, & G. Johnsen (Eds.), *Phytoplankton Pigments: Characterization,*  
1299 *Chemotaxonomy, and Application in Oceanography* (pp. 3-77). Cambridge, United Kingdom: Cambridge  
1300 University Press

1301 Johnson, T.R., Beard, K., Brady, D.C., Byron, C.J., Cleaver, C., Duffy, K., Keeney, N., Kimble, M., Miller, M.,  
1302 Moeykens, S., Teisl, M., van Walsum, G.P., & Yuan, J. (2019). A Social-Ecological System Framework for  
1303 Marine Aquaculture Research. *Sustainability*, 11, 2522

1304 Johnson, Z.I., & Martiny, A.C. (2015). Techniques for Quantifying Phytoplankton Biodiversity. *Annual*  
1305 *Review of Marine Science*, 7, 299-324

1306 Jones, E.M., Baird, M.E., Mongin, M., Parslow, J., Skerratt, J., Lovell, J., Margvelashvili, N., Matear, R.J.,  
1307 Wild-Allen, K., & Robson, B. (2016). Use of remote-sensing reflectance to constrain a data assimilating  
1308 marine biogeochemical model of the Great Barrier Reef. *Biogeosciences*, 13, 6441-6469

1309 Kahru, M., Anderson, C., Barton, A.D., Carter, M.L., Catlett, D., Send, U., Sosik, H.M., Weiss, E.L., &  
1310 Mitchell, B.G. (2021). Satellite detection of dinoflagellate blooms off California by UV reflectance ratios.  
1311 *Elem Sci Anth*, 9, 00157

1312 Kahru, M., & Mitchell, B. (1998). Spectral reflectance and absorption of a massive red tide off southern  
1313 California. *Journal of Geophysical Research*, *103*, 21601-21609

1314 Karlson, B., Godhe, A., Cusack, C., & Bresnan, E. (2010). Introduction to methods for quantitative  
1315 phytoplankton analysis. *Microscopic and molecular methods for quantitative phytoplankton analysis*, IOC  
1316 Manual and Guides No. 55, UNESCO, Paris. 110p.

1317 Kavanaugh, M. T., Bell, T., Catlett, D., Cimino, M. A., Doney, S. C., Klajbor, W., Messie, M., Montes, E.,  
1318 Muller Karger F.E., Otis, D., Santora, J.A., Schroeder, I.D., Trinanés, J., & Siegel, D. A. (2021). Satellite  
1319 remote sensing and the marine biodiversity observation network. *Oceanography*, *34*(2), 62-79.

1320 Kerr, T., Clark, J.R., Fileman, E.S., Widdicombe, C.E., & Pugeault, N. (2020). Collaborative Deep Learning  
1321 Models to Handle Class Imbalance in FlowCam Plankton Imagery. *IEEE Access*, *8*, 170013-170032

1322 Kirkpatrick, G.J., Millie, D.F., Moline, M.A., & Schofield, O. (2000). Optical discrimination of a  
1323 phytoplankton species in natural mixed populations. *Limnology and Oceanography*, *45*, 467-471

1324 Kostadinov, T., Siegel, D., & Maritorena, S. (2009). Retrieval of the particle size distribution from satellite  
1325 ocean color observations. *Journal of Geophysical Research: Oceans*, *114*

1326 Kostadinov, T., Siegel, D., & Maritorena, S. (2010). Global variability of phytoplankton functional types  
1327 from space: assessment via the particle size distribution. *Biogeosciences*, *7*, 3239-3257

1328 Kostadinov, T.S. (2016). Carbon-based phytoplankton size classes retrieved via ocean color estimates of  
1329 the particle size distribution. *Ocean Science*, *12*, 561

1330 Kostadinov, T.S., Cabré, A., Vedantham, H., Marinov, I., Bracher, A., Brewin, R.J., Bricaud, A., Hirata, T.,  
1331 Hirawake, T., & Hardman-Mountford, N.J. (2017). Inter-comparison of phytoplankton functional type  
1332 phenology metrics derived from ocean color algorithms and earth system models. *Remote Sensing of  
1333 Environment*, *190*, 162-177

1334 Kostadinov, T.S., Robertson Lain, L., Kong, C.E., Zhang, X., Maritorena, S., Bernard, S., Loisel, H., Jorge,  
1335 D.S.F., Kochetkova, E., Roy, S., Jonsson, B., Martinez-Vicente, V., & Sathyendranath, S. (2022). Ocean  
1336 Color Algorithm for the Retrieval of the Particle Size Distribution and Carbon-Based Phytoplankton Size  
1337 Classes Using a Two-Component Coated-Spheres Backscattering Model. *EGUsphere*, *2022*, 1-38

1338 Kostakis, I., Twardowski, M., Roesler, C., Röttgers, R., Stramski, D., McKee, D., Tonizzo, A., & Drapeau, S.  
1339 (2021). Hyperspectral optical absorption closure experiment in complex coastal waters. *Limnology and  
1340 Oceanography: Methods*, *19*, 589-625

1341 Kramer, S.J., Roesler, C.S., & Sosik, H.M. (2018). Bio-optical discrimination of diatoms from other  
1342 phytoplankton in the surface ocean: Evaluation and refinement of a model for the Northwest Atlantic.  
1343 *Remote Sensing of Environment*, *217*, 126-143

1344 Kramer, S.J., & Siegel, D.A. (2019). How Can Phytoplankton Pigments Be Best Used to Characterize  
1345 Surface Ocean Phytoplankton Groups for Ocean Color Remote Sensing Algorithms? *Journal of  
1346 Geophysical Research: Oceans*, *124*, 7557-7574

1347 Kramer, S.J., Siegel, D.A., & Graff J.R. (2020). Phytoplankton Community Composition Determined From  
1348 Co-variability Among Phytoplankton Pigments From the NAAMES Field Campaign. *Frontiers in Marine  
1349 Science*, *7*

1350 Kramer, S.J., Siegel, D.A., Maritorena, S., & Catlett, D. (2022). Modeling surface ocean phytoplankton  
1351 pigments from hyperspectral remote sensing reflectance on global scales. *Remote Sensing of  
1352 Environment*, *270*, 112879

1353 Kudela, R.M., Palacios, S.L., Austerberry, D.C., Accorsi, E.K., Guild, L.S., & Torres-Perez, J. (2015).  
1354 Application of hyperspectral remote sensing to cyanobacterial blooms in inland waters. *Remote Sensing  
1355 of Environment*, *167*, 196-205

1356 Lange, P. K., Brewin, R. J., Dall'Olmo, G., Tarran, G. A., Sathyendranath, S., Zubkov, M., & Bouman, H. A.  
1357 (2018). Scratching beneath the surface: A model to predict the vertical distribution of Prochlorococcus  
1358 using remote sensing. *Remote Sensing*, *10*, 847

1359 Lange, P.K., Jeremy Werdell, P., Erickson, Z.K., Dall’Olmo, G., Brewin, R.J.W., Zubkov, M.V., Tarran, G.A.,  
1360 Bouman, H.A., Slade, W.H., Craig, S.E., Poulton, N.J., Bracher, A., Lomas, M.W., & Cetinić, I. (2020).  
1361 Radiometric approach for the detection of picophytoplankton assemblages across oceanic fronts. *Optics*  
1362 *Express*, *28*, 25682-25705

1363 Lee, Z., Carder, K., Arnone, R. and He, M. (2007). Determination of primary spectral bands for remote  
1364 sensing of aquatic environments. *Sensors*, *7*, 3428-3441

1365 Le Quéré, C., Takahashi, T., Buitenhuis, E.T., Rödenbeck, C., & Sutherland, S.C. (2010). Impact of climate  
1366 change and variability on the global oceanic sink of CO<sub>2</sub>. *Global Biogeochemical Cycles*, *24*, n/a-n/a

1367 LeGresley, M., & McDermott, G. (2010). Counting chamber methods for quantitative phytoplankton  
1368 analysis-haemocytometer, Palmer-Maloney cell and Sedgewick-Rafter cell. *UNESCO (IOC manuals and*  
1369 *guides)*, 25-30

1370 Lehmann, M.K., Gurlin, D., Pahlevan, N., Alikas, K., ... & Yue, L. (2023). GLORIA - A globally representative  
1371 hyperspectral in situ dataset for optical sensing of water quality. *Scientific Data*, *10*.

1372 Lepesteur, M., Martin, J. M., & Fleury, A. (1993). A comparative study of different preservation methods  
1373 for phytoplankton cell analysis by flow cytometry. *Marine Ecology Progress Series*, *93*, 55–63.

1374 Lekki, J., Ruberg, S., Binding, C., Anderson, R., & Vander Woude, A. (2019). Airborne hyperspectral and  
1375 satellite imaging of harmful algal blooms in the Great Lakes Region: Successes in sensing algal blooms.  
1376 *Journal of Great Lakes Research*, *45*, 405-412

1377 Li, Z., Li, L., Song, K., & Cassar, N. (2013). Estimation of Phytoplankton Size Fractions Based on Spectral  
1378 Features of Remote Sensing Ocean Color Data. *Journal of Geophysical Research: Oceans*, *118*, n/a-n/a

1379 Lin, Y., Gifford, S., Ducklow, H., Schofield, O., & Cassar, N. (2019). Towards quantitative microbiome  
1380 community profiling using internal standards. *Applied and Environmental Microbiology*, *85*, 1-14

1381 Liu, Y., Boss, E., Chase, A., Xi, H., Zhang, X., Röttgers, R., Pan, Y., & Bracher, A. (2019). Retrieval of  
1382 phytoplankton pigments from underway spectrophotometry in the Fram Strait. *Remote Sensing*, *11*, 318

1383 Llewellyn, C.A., & Airs, R.L. (2010). Distribution and abundance of MAAs in 33 species of microalgae  
1384 across 13 classes. *Marine Drugs*, *8*, 1273-1291

1385 Lohrenz, S.E., Weidemann, A.D., & Tuel, M. (2003). Phytoplankton spectral absorption as influenced by  
1386 community size structure and pigment composition. *Journal of Plankton Research*, *25*, 35-61

1387 Loisel, H., Duforet, L., Dessailly, D., Chami, M., & Dubuisson, P. (2008). Investigation of the variations in  
1388 the water leaving polarized reflectance from the POLDER satellite data over two biogeochemical  
1389 contrasted oceanic areas. *Optics Express*, *16*, 12905-12918

1390 Loisel, H., Stramski, D., Dessailly, D., Jamet, C., Li, L., & Reynolds, R.A. (2018). An inverse model for  
1391 estimating the optical absorption and backscattering coefficients of seawater from remote-sensing  
1392 reflectance over a broad range of oceanic and coastal marine environments. *Journal of Geophysical*  
1393 *Research: Oceans*, *123*, 2141-2171

1394 Lombard, F., Boss, E., Waite, A.M., Vogt, M., Uitz, J., Stemmann, L., Sosik, H.M., Schulz, J., Romagnan, J.-  
1395 B., Picheral, M., Pearlman, J., Ohman, M.D., Niehoff, B., Möller, K.O., Miloslavich, P., Lara-Lpez, A.,  
1396 Kudela, R., Lopes, R.M., Kiko, R., Karp-Boss, L., Jaffe, J.S., Iversen, M.H., Irisson, J.-O., Fennel, K., Hauss,  
1397 H., Guidi, L., Gorsky, G., Giering, S.L.C., Gaube, P., Gallager, S., Dubelaar, G., Cowen, R.K., Carlotti, F.,  
1398 Briseño-Avena, C., Berline, L., Benoit-Bird, K., Bax, N., Batten, S., Ayata, S.D., Artigas, L.F., & Appeltans,  
1399 W. (2019). Globally Consistent Quantitative Observations of Planktonic Ecosystems. *Frontiers in Marine*  
1400 *Science*, *6*

1401 Losa, S.N., Soppa, M.A., Dinter, T., Wolanin, A., Brewin, R.J.W., Bricaud, A., Oelker, J., Peeken, I., Gentili,  
1402 B., Rozanov, V., & Bracher, A. (2017). Synergistic Exploitation of Hyper- and Multi-Spectral Precursor  
1403 Sentinel Measurements to Determine Phytoplankton Functional Types (SynSenPFT). *Frontiers in Marine*  
1404 *Science*, *4*

1405 Lubac, B., Loisel, H., Guiselin, N., Astoreca, R., Artigas, L.F., & Meriaux, X. (2008). Hyperspectral and  
1406 multispectral ocean color inversions to detect *Phaeocystis globosa* blooms in coastal waters. *Journal of*  
1407 *Geophysical Research-Oceans*, *113*

1408 Lucke, R.L., Corson, M., McGlothlin, N.R., Butcher, S.D., Wood, D.L., Korwan, D.R., Li, R.R., Snyder, W.A.,  
1409 Davis, C.O., & Chen, D.T. (2011). Hyperspectral Imager for the Coastal Ocean: instrument description and  
1410 first images. *Applied Optics*, *50*, 1501-1516

1411 Lundholm, N., Churro, C., Fraga, S., Hoppenrath, M., Iwataki, M., Larsen, J., Mertens, K., Moestrup, Ø., &  
1412 Zingone, A. (2009). IOC-UNESCO Taxonomic Reference List of Harmful Micro Algae. Accessed at  
1413 <https://www.marinespecies.org/hab> on 2023-03-14.

1414 Mackey, M.D., Mackey, D.J., Higgins, H.W., & Wright, S.W. (1996). CHEMTAX - A program for estimating  
1415 class abundances from chemical markers: Application to HPLC measurements of phytoplankton. *Marine*  
1416 *Ecology-Progress Series*, *144*, 265-283

1417 Mao, Z., Stuart, V., Pan, D., Chen, J., Gong, F., Huang, H., & Zhu, Q. (2010). Effects of phytoplankton  
1418 species composition on absorption spectra and modeled hyperspectral reflectance. *Ecological*  
1419 *Informatics*, *5*, 359-366

1420 Marie, D., Rigaut-Jalabert, F., & Vaultot, D. (2014). An improved protocol for flow cytometry analysis of  
1421 phytoplankton cultures and natural samples. *Cytometry Part A*, *85*, 962-968

1422 Martins, J.V., Tanré, D., Remer, L., Kaufman, Y., Mattoo, S., & Levy, R. (2002). MODIS cloud screening for  
1423 remote sensing of aerosols over oceans using spatial variability. *Geophysical Research Letters*, *29*, MOD4-  
1424 1-MOD4-4

1425 McAlice, B.J. (1971). Phytoplankton Sampling with the Sedgwick-Rafter Cell. *Limnology and*  
1426 *Oceanography*, *16*, 19-28

1427 McCabe, R.M., Hickey, B.M., Kudela, R.M., Lefebvre, K.A., Adams, N.G., Bill, B.D., Gulland, F.M.D.,  
1428 Thomson, R.E., Cochlan, W.P., & Trainer, V.L. (2016). An unprecedented coastwide toxic algal bloom  
1429 linked to anomalous ocean conditions. *Geophysical Research Letters*, *43*, 10,366-310,376

1430 McClain, C.R., Franz, B.A., & Werdell, P.J. (2022). Genesis and Evolution of NASA's Satellite Ocean Color  
1431 Program. *Frontiers in Remote Sensing*, *3*

1432 McKibben, S. M., Peterson, W., Wood, A. M., Trainer, V. L., Hunter, M., & White, A. E. (2017). Climatic  
1433 regulation of the neurotoxin domoic acid. *Proceedings of the National Academy of Sciences*, *114*, 239-  
1434 244

1435 McKinna, L.I. (2015). Three decades of ocean-color remote-sensing *Trichodesmium* spp. in the World's  
1436 oceans: A review. *Progress in Oceanography*, *131*, 177-199

1437 McKinna, L.I.W., Cetinić, I., Chase, A.P., & Werdell, P.J. (2019). Approach for Propagating Radiometric  
1438 Data Uncertainties Through NASA Ocean Color Algorithms. *Frontiers in Earth Science*, *7*

1439 McKinna, L.I.W., Cetinić, I., & Werdell, P.J. (2021). Development and Validation of an Empirical Ocean  
1440 Color Algorithm with Uncertainties: A Case Study with the Particulate Backscattering Coefficient. *Journal*  
1441 *of Geophysical Research: Oceans*, *126*, e2021JC017231

1442 McKinna, L.I.W., Furnas, M.J., & Ridd, P.V. (2011). A simple, binary classification algorithm for the  
1443 detection of *Trichodesmium* spp. within the Great Barrier Reef using MODIS imagery. *Limnology and*  
1444 *Oceanography: Methods*, *9*, 50-66

1445 Meier, W.N., Perovich, D., Farrell, S., Haas, C., Hendricks, S., Petty, A.A., Webster, M., Divine, D., Gerland,  
1446 S., Kaleschke, L., Ricker, R., Steer, A., Tian-Kunze, X., Tschudi, M., & Wood, K. (2021). Sea Ice. In T.A.  
1447 Moon, M.L. Druckenmiller, & R.L. Thoman (Eds.), *Arctic Report Card 2021*

1448 Menden-Deuer, S., & Lessard, E.J. (2000). Carbon to volume relationships for dinoflagellates, diatoms  
1449 and other protist plankton. *Limnology and Oceanography*, *45*, 569-579

1450 Michalak, A.M. (2016). Study role of climate change in extreme threats to water quality. *Nature*, *535*,  
1451 349-350

1452 Millie, D.F., Schofield, O.M., Kirkpatrick, G.J., Johnsen, G., Tester, P.A., & Vinyard, B.T. (1997). Detection  
1453 of harmful algal blooms using photopigments and absorption signatures: A case study of the Florida red  
1454 tide dinoflagellate, *Gymnodinium breve*. *Limnology and Oceanography*, *42*, 1240-1251

1455 Mitra, A., Flynn, K.J., Tillmann, U., Raven, J.A., Caron, D., Stoecker, D.K., Not, F., Hansen, P.J., Hallegraeff,  
1456 G., Sanders, R., Wilken, S., McManus, G., Johnson, M., Pitta, P., Våge, S., Berge, T., Calbet, A., Thingstad,  
1457 F., Jeong, H.J., Burkholder, J., Glibert, P.M., Granéli, E., & Lundgren, V. (2016). Defining Planktonic Protist  
1458 Functional Groups on Mechanisms for Energy and Nutrient Acquisition: Incorporation of Diverse  
1459 Mixotrophic Strategies. *Protist*, *167*, 106-120

1460 Mobley, C. (Ed.) (2022). *The Oceanic Optics Book*. Dartmouth, NS, Canada: International Ocean Colour  
1461 Coordinating Group (IOCCG)

1462 Moore, T.S., & Brown, C.W. (2020). Incorporating environmental data in abundance-based algorithms for  
1463 deriving phytoplankton size classes in the Atlantic Ocean. *Remote Sensing of Environment*, *240*, 111689

1464 Moore, T.S., Dowell, M.D., & Franz, B.A. (2012). Detection of coccolithophore blooms in ocean color  
1465 satellite imagery: A generalized approach for use with multiple sensors. *Remote Sensing of Environment*,  
1466 *117*, 249-263

1467 Morel, A., & Berthon, J. F. (1989). Surface pigments, algal biomass profiles, and potential production of  
1468 the euphotic layer: Relationships reinvestigated in view of remote-sensing applications. *Limnology and*  
1469 *oceanography*, *34*, 1545-1562.

1470 Morel, A., & Prieur, L. (1977). Analysis of variation in ocean color. *Limnology and Oceanography*, *22*, 709-  
1471 722

1472 Mouw, C.B., Hardman-Mountford, N.J., Alvain, S., Bracher, A., Brewin, R.J.W., Bricaud, A., Ciotti, A.M.,  
1473 Devred, E., Fujiwara, A., Hirata, T., Hirawake, T., Kostadinov, T.S., Roy, S., & Uitz, J. (2017). A Consumer's  
1474 Guide to Satellite Remote Sensing of Multiple Phytoplankton Groups in the Global Ocean. *Frontiers in*  
1475 *Marine Science*, *4*

1476 Mouw, C.B., & Yoder, J.A. (2010). Optical determination of phytoplankton size composition from global  
1477 SeaWiFS imagery. *Journal of Geophysical Research: Oceans*, *115*

1478 Muller-Karger, F.E., Hestir, E., Ade, C., Turpie, K., Roberts, D.A., ... & Jetz, W. (2018). Satellite sensor  
1479 requirements for monitoring essential biodiversity variables of coastal ecosystems. *Ecological*  
1480 *Applications*, *28*, 749-760

1481 Muller-Karger, F. E., Miloslavich, P., Bax, N. J., Simmons, S., Costello, M. J., Sousa Pinto, I., ... & Geller, G.  
1482 (2018). Advancing marine biological observations and data requirements of the complementary essential  
1483 ocean variables (EOVs) and essential biodiversity variables (EBVs) frameworks. *Frontiers in Marine*  
1484 *Science*, 211.

1485 Nardelli, S.C., Gray, P.C., Stammerjohn, S.E., & Schofield, O. (2023). Characterizing coastal phytoplankton  
1486 seasonal succession patterns on the West Antarctic Peninsula. *Limnology and Oceanography*.

1487 NASA (2010). Responding to the Challenge of Climate and Environmental Change: NASA's Plan for a  
1488 Climate-Centric Architecture for Earth Observations and Applications from Space. (p. 48)

1489 National Academies of Sciences, Engineering, and Medicine (2022). A research strategy for ocean-based  
1490 carbon dioxide removal and sequestration. In. Washington, DC The National Academies Press.

1491 National Research Council (2007). Earth science and applications from space: National imperatives for  
1492 the next decade and beyond. *The National Academies Press, Washington, DC*, *10*, 11820

1493 Neeley, A., Beaulieu, S., Proctor, C., Cetinic, I., Futrelle, J., Soto Ramos, I., Sosik, H., Devred, E., Karp-Boss,  
1494 L., & Picheral, M. (2021). Standards and practices for reporting plankton and other particle observations  
1495 from images. In, *Ocean Carbon and Biogeochemistry Publications: Ocean Carbon and Biogeochemistry*

1496 Neeley, A., Harris, L., & Frey, K. (2018). Unraveling Phytoplankton Community Dynamics in the Northern  
1497 Chukchi Sea Under Sea-Ice-Covered and Sea-Ice-Free Conditions. *Geophysical Research Letters*, *45*, 7663-  
1498 7671

1499 Neeley, A.R., Lomas, M.W., Mannino, A., Thomas, C., & Vandermeulen, R. (2022). Impact of Growth  
1500 Phase, Pigment Adaptation, and Climate Change Conditions on the Cellular Pigment and Carbon Content  
1501 of Fifty-One Phytoplankton Isolates. *Journal of Phycology*, *58*, 669-690  
1502 Neeley, A.R., Soto-Ramos, I., & Proctor, C. (2023). Standards and Best Practices for Reporting Flow  
1503 Cytometry Observations: a technical manual, Version 1.1. Greenbelt, MD., NASA Goddard Space Flight  
1504 Center, 31pp.  
1505 O'Shea, R.E., Pahlevan, N., Smith, B., Bresciani, M., Egerton, T., Giardino, C., Li, L., Moore, T., Ruiz-Verdu,  
1506 A., Ruberg, S., Simis, S.G.H., Stumpf, R., & Vaičiūtė, D. (2021). Advancing cyanobacteria biomass  
1507 estimation from hyperspectral observations: Demonstrations with HICO and PRISMA imagery. *Remote  
1508 Sensing of Environment*, *266*, 112693  
1509 Olson, R.J., Chisholm, S.W., Zettler, E.R., & Armbrust, E.V. (1988). Analysis of Synechococcus pigment  
1510 types in the sea using single and dual beam flow cytometry. *Deep Sea Research Part A. Oceanographic  
1511 Research Papers*, *35*, 425-440  
1512 Olson, R.J., & Sosik, H.M. (2007). A submersible imaging-in-flow instrument to analyze nano-and  
1513 microplankton: Imaging FlowCytobot. *Limnology and Oceanography: Methods*, *5*, 195-203  
1514 O'Reilly, John E., et al. "Ocean color chlorophyll algorithms for SeaWiFS." *Journal of Geophysical  
1515 Research: Oceans* 103.C11 (1998): 24937-24953.  
1516 Orenstein, E.C., Ayata, S.-D., Maps, F., Becker, É.C., Benedetti, F., Biard, T., ...& Irisson, J.-O. (2022).  
1517 Machine learning techniques to characterize functional traits of plankton from image data. *Limnology  
1518 and Oceanography*, *67*, 1647-1669  
1519 Organelli, E., Dall'Olmo, G., Brewin, R.J.W., Tarran, G.A., Boss, E., & Bricaud, A. (2018). The open-ocean  
1520 missing backscattering is in the structural complexity of particles. *Nature Communications*, *9*, 5439  
1521 PACE mission (2020). Plankton, Aerosol, Cloud, ocean Ecosystem (PACE) mission PACE Science Data  
1522 Product Validation Plan. NASA GSFC, Greenbelt.  
1523 Pahlevan, N., Smith, B., Binding, C., Gurlin, D., Li, L., Bresciani, M., & Giardino, C. (2021). Hyperspectral  
1524 retrievals of phytoplankton absorption and chlorophyll-a in inland and nearshore coastal waters. *Remote  
1525 Sensing of Environment*, *253*, 112200  
1526 Palacios, S.L., Kudela, R.M., Guild, L.S., Negrey, K.H., Torres-Perez, J., & Broughton, J. (2015). Remote  
1527 sensing of phytoplankton functional types in the coastal ocean from the HypSPRI Preparatory Flight  
1528 Campaign. *Remote Sensing of Environment*, *167*, 269-280  
1529 Palacz, A., St. John, M., Brevin, R., Hirata, T., & Gregg, W. (2013). Distribution of phytoplankton functional  
1530 types in high-nitrate low-chlorophyll waters in a new diagnostic ecological indicator model.  
1531 *Biogeosciences*, *10*, 7553-7574  
1532 Pan, X., Mannino, A., Russ, M.E., Hooker, S.B., & Harding Jr, L.W. (2010). Remote sensing of  
1533 phytoplankton pigment distribution in the United States northeast coast. *Remote Sensing of  
1534 Environment*, *114*, 2403-2416  
1535 Parada, A.E., Needham, D.M., & Fuhrman, J.A. (2016). Every base matters: assessing small subunit rRNA  
1536 primers for marine microbiomes with mock communities, time series and global field samples.  
1537 *Environmental microbiology*, *18*, 1403-1414  
1538 Picheral, M., Guidi, L., Stemmann, L., Karl, D.M., Iddaoud, G., & Gorsky, G. (2010). The Underwater Vision  
1539 Profiler 5: An advanced instrument for high spatial resolution studies of particle size spectra and  
1540 zooplankton. *Limnology and Oceanography: Methods*, *8*, 462-473  
1541 Poulin, C., Zhang, X., Yang, P., & Huot, Y. (2018). Diel variations of the attenuation, backscattering and  
1542 absorption coefficients of four phytoplankton species and comparison with spherical, coated spherical  
1543 and hexahedral particle optical models. *Journal of Quantitative Spectroscopy and Radiative Transfer*,  
1544 *217*, 288-304  
1545 Racault, M.-F., Sathyendranath, S., Brewin, R.J.W., Raitsos, D.E., Jackson, T., & Platt, T. (2017). Impact of  
1546 El Niño Variability on Oceanic Phytoplankton. *Frontiers in Marine Science*, *4*

1547 Raitso, D.E., Lavender, S.J., Maravelias, C.D., Haralabous, J., Richardson, A.J., & Reid, P.C. (2008).  
1548 Identifying four phytoplankton functional types from space: An ecological approach. *Limnology and*  
1549 *Oceanography*, *53*, 605-613

1550 Rasconi, S., Gall, A., Winter, K., & Kainz, M.J. (2015). Increasing Water Temperature Triggers Dominance  
1551 of Small Freshwater Plankton. *PLoS ONE*, *10*, e0140449

1552 Remer, L.A., Knobelspiesse, K., Zhai, P.-W., Xu, F., Kalashnikova, O.V., Chowdhary, J., Hasekamp, O.,  
1553 Dubovik, O., Wu, L., Ahmad, Z., Boss, E., Cairns, B., Coddington, O., Davis, A.B., Dierssen, H.M., Diner,  
1554 D.J., Franz, B., Frouin, R., Gao, B.-C., Ibrahim, A., Levy, R.C., Martins, J.V., Omar, A.H., & Torres, O. (2019).  
1555 Retrieving Aerosol Characteristics From the PACE Mission, Part 2: Multi-Angle and Polarimetry. *Frontiers*  
1556 *in Environmental Science*, *7*

1557 Rêve-Lamarque, A.-H., Alvain, S., Racault, M.-F., Dessailly, D., Guiselin, N., Jamet, C., Vantrepotte, V., &  
1558 Beaugrand, G. (2017). Estimation of the potential detection of diatom assemblages based on ocean color  
1559 radiance anomalies in the North Sea. *Frontiers in Marine Science*, *4*, 408

1560 Rivero-Calle, S., Gnanadesikan, A., Del Castillo, C.E., Balch, W.M., & Guikema, S.D. (2015). Multidecadal  
1561 increase in North Atlantic coccolithophores and the potential role of rising CO<sub>2</sub>. *Science*,  
1562 *350*, 1533-1537

1563 Roelke, D., Kennedy, C., & Weidemann, A. (1999). Use of discriminant and fourth-derivative analyses  
1564 with high-resolution absorption spectra for phytoplankton research: Limitations at varied signal-to-noise  
1565 ratio and spectral resolution. *Gulf of Mexico Science*, *17*, 75-86

1566 Roesler, C.S., & Boss, E. (2003). Spectral beam attenuation coefficient retrieved from ocean color  
1567 inversion. *Geophysical Research Letters*, *30*, 1468

1568 Rose, J.M., Caron, D.A., Sieracki, M.E., & Poulton, N. (2004). Counting heterotrophic nanoplanktonic  
1569 protists in cultures and aquatic communities by flow cytometry. *Aquatic Microbial Ecology*, *34*, 263-277

1570 Rousseaux, C.S., & Gregg, W.W. (2012). Climate variability and phytoplankton composition in the Pacific  
1571 Ocean. *Journal of Geophysical Research: Oceans*, *117*, n/a-n/a

1572 Roy, S., Sathyendranath, S., Bouman, H., & Platt, T. (2013). The global distribution of phytoplankton size  
1573 spectrum and size classes from their light-absorption spectra derived from satellite data. *Remote Sensing*  
1574 *of Environment*, *139*, 185-197

1575 Ryan, J.P., Chavez, F.P., & Bellingham, J.G. (2005). Physical-biological coupling in Monterey Bay,  
1576 California: topographic influences on phytoplankton ecology. *Marine Ecology-Progress Series*, *287*, 23-32

1577 Ryan, J.P., Davis, C.O., Tuffillaro, N.B., Kudela, R.M., & Gao, B.-C. (2014). Application of the Hyperspectral  
1578 Imager for the Coastal Ocean to Phytoplankton Ecology Studies in Monterey Bay, CA, USA. *Remote*  
1579 *Sensing*, *6*, 1007-1025

1580 Sadeghi, A., Dinter, T., Vountas, M., Taylor, B., Altenburg-Soppa, M., & Bracher, A. (2012). Remote  
1581 sensing of coccolithophore blooms in selected oceanic regions using the PhytoDOAS method applied to  
1582 hyper-spectral satellite data. *Biogeosciences*, *9*, 2127-2143

1583 Sathyendranath, S., Watts, L., Devred, E., Platt, T., Caverhill, C., & Maass, H. (2004). Discrimination of  
1584 diatoms from other phytoplankton using ocean-colour data. *Marine Ecology-Progress Series*, *272*, 59-68

1585 Satinsky, B.M., Gifford, S.M., Crump, B.C., & Moran, M.A. (2013). Chapter Twelve - Use of Internal  
1586 Standards for Quantitative Metatranscriptome and Metagenome Analysis. In E.F. DeLong (Ed.), *Methods*  
1587 *in Enzymology* (pp. 237-250): Academic Press

1588 Sato, M., Takeda, S., & Furuya, K. (2006). Effects of long-term sample preservation on flow cytometric  
1589 analysis of natural populations of pico-and nanophytoplankton. *Journal of Oceanography*, *62*, 903-908

1590 Sayer, A.M., Lelli, L., Cairns, B., van Dienenhoven, B., Ibrahim, A., Knobelspiesse, K., Korke, S., & Werdell,  
1591 P.J. (2022). The CHROMA cloud top pressure retrieval algorithm for the Plankton, Aerosol, Cloud, ocean  
1592 Ecosystem (PACE) satellite mission. *Atmos. Meas. Tech. Discuss.*, *2022*, 1-40

1593 Schaeffer, B.A., Loftin, K.A., Stumpf, R.P., & Werdell, P.J. (2015). Agencies collaborate, develop a  
1594 cyanobacteria assessment network. *Eos, Earth and Space Science News*, 96

1595 Schoening, T., Durden, J. M., Faber, C., Felden, J., Heger, K., Hoving, H. J. T., ... & Zurowietz, M. (2022).  
1596 Making marine image data FAIR. *Scientific data*, 9, 414

1597 Schofield, O., Brown, M., Kohut, J., Nardelli, S., Saba, G., Waite, N., & Ducklow, H. (2018). Changes in the  
1598 upper ocean mixed layer and phytoplankton productivity along the West Antarctic Peninsula.  
1599 *Philosophical Transactions of the Royal Society A: Mathematical, Physical and Engineering Sciences*, 376,  
1600 20170173

1601 Shaju, S.S., Minu, P., Srikanth, A.S., Ashraf, P.M., Vijayan, A.K., & Meenakumari, B. (2015). Decomposition  
1602 study of in vivo phytoplankton absorption spectra aimed at identifying the pigments and the  
1603 phytoplankton group in complex case 2 coastal waters of the Arabian Sea. *Oceanological and*  
1604 *Hydrobiological Studies*, 44, 282-293

1605 Shulman, I., Frolov, S., Anderson, S., Penta, B., Gould, R., Sakalaukus, P., & Ladner, S. (2013). Impact of  
1606 bio-optical data assimilation on short-term coupled physical, bio-optical model predictions. *Journal of*  
1607 *Geophysical Research: Oceans*, 118, 2215-2230

1608 Siegel, D.A., Behrenfeld, M.J., Maritorena, S., McClain, C.R., Antoine, D., ...& Yoder, J.A. (2013). Regional  
1609 to global assessments of phytoplankton dynamics from the SeaWiFS mission. *Remote Sensing of*  
1610 *Environment*, 135, 77-91

1611 Siegel, D.A., DeVries, T., Cetinić, I., & Bisson, K.M. (2023). Quantifying the Ocean's Biological Pump and Its  
1612 Carbon Cycle Impacts on Global Scales. *Annual Review of Marine Science*, 15, null

1613 Sieracki, C.K., Sieracki, M.E., & Yentsch, C.S. (1998). An imaging-in-flow system for automated analysis of  
1614 marine microplankton. *Marine Ecology Progress Series*, 285-296

1615 Skákala, J., Ford, D., Brewin, R.J.W., McEwan, R., Kay, S., Taylor, B., de Mora, L., & Ciavatta, S. (2018). The  
1616 Assimilation of Phytoplankton Functional Types for Operational Forecasting in the Northwest European  
1617 Shelf. *Journal of Geophysical Research: Oceans*, 123, 5230-5247

1618 Smith, M.E., & Bernard, S. (2020). Satellite Ocean Color Based Harmful Algal Bloom Indicators for  
1619 Aquaculture Decision Support in the Southern Benguela. *Frontiers in Marine Science*, 7

1620 Snyder, J., Boss, E., Weatherbee, R., Thomas, A.C., Brady, D., & Newell, C. (2017). Oyster Aquaculture Site  
1621 Selection Using Landsat 8-Derived Sea Surface Temperature, Turbidity, and Chlorophyll a. *Frontiers in*  
1622 *Marine Science*, 4

1623 Soppa, M.A., Hirata, T., Silva, B., Dinter, T., Peeken, I., Wiegmann, S., & Bracher, A. (2014). Global  
1624 Retrieval of Diatom Abundance Based on Phytoplankton Pigments and Satellite Data. *Remote Sensing*, 6,  
1625 10089-10106

1626 Sosik, H.M., Olson, R.J., Neubert, M.G., Shalapyonok, A., & Solow, A.R. (2003). Growth rates of coastal  
1627 phytoplankton from time-series measurements with a submersible flow cytometer. *Limnology and*  
1628 *Oceanography*, 48, 1756-1765

1629 Soto, I.M., Cannizzaro, J., Muller-Karger, F.E., Hu, C., Wolny, J., & Goldgof, D. (2015). Evaluation and  
1630 optimization of remote sensing techniques for detection of *Karenia brevis* blooms on the West Florida  
1631 Shelf. *Remote Sensing of Environment*, 170, 239-254

1632 Stramski, D., Bricaud, A., & Morel, A. (2001). Modeling the inherent optical properties of the ocean based  
1633 on the detailed composition of planktonic community. *Applied Optics* 40, 2929–2945.

1634 Stramski, D. & Kiefer, D. A. (1991). Light scattering by microorganisms in the open ocean. *Progress in*  
1635 *Oceanography* 28, 343–383

1636 Stramski, D. & Reynolds, R.A. (1993). Diel variations in the optical properties of a marine diatom.  
1637 *Limnology and Oceanography*, 38, 1347–1364

1638 Stramski, D., Shalapyonok, A. & R. A. Reynolds (1995). Optical characterization of the oceanic unicellular  
1639 cyanobacterium *Synechococcus* grown under a day-night cycle in natural irradiance. *Journal of*  
1640 *Geophysical Research*, 100, 13295–13307

1641 Stramska, M., & Stramski, D. (2005). Effects of a nonuniform vertical profile of chlorophyll concentration  
1642 on remote-sensing reflectance of the ocean. *Applied Optics*, 44, 1735-1747

1643 Subramaniam, A., Brown, C.W., Hood, R.R., Carpenter, E.J., & Capone, D.G. (2001). Detecting  
1644 Trichodesmium blooms in SeaWiFS imagery. *Deep Sea Research Part II: Topical Studies in Oceanography*,  
1645 *49*, 107-121

1646 Subramaniam, A., & Carpenter, E.J. (1994). An empirically derived protocol for the detection of blooms  
1647 of the marine cyanobacterium Trichodesmium using CZCS imagery. *International Journal of Remote*  
1648 *Sensing*, *15*, 1559-1569

1649 Sun, X., Shen, F., Brewin, R.J., Li, M., & Zhu, Q. (2022). Light absorption spectra of naturally mixed  
1650 phytoplankton assemblages for retrieval of phytoplankton group composition in coastal oceans.  
1651 *Limnology and Oceanography*, *67*, 946-961

1652 Swalwell, J.E., Ribalet, F., & Armbrust, E.V. (2011). SeaFlow: A novel underway flow-cytometer for  
1653 continuous observations of phytoplankton in the ocean. *Limnology and Oceanography: Methods*, *9*, 466-  
1654 477

1655 Sydor, M., Gould, R.W., Arnone, R.A., Haltrin, V.I., & Goode, W. (2004). Uniqueness in remote sensing of  
1656 the inherent optical properties of ocean water. *Applied Optics*, *43*, 2156-2162

1657 Taylor, B.B., Taylor, M.H., Dinter, T., & Bracher, A. (2013). Estimation of relative phycoerythrin  
1658 concentrations from hyperspectral underwater radiance measurements—A statistical approach. *Journal*  
1659 *of Geophysical Research: Oceans*, *118*, 2948-2960

1660 Thompson, P.A., & Carstensen, J. (2022). Global observing for phytoplankton? A perspective. *Journal of*  
1661 *Plankton Research*

1662 Thyssen, M., Alvain, S., Lefèbvre, A., Dessailly, D., Rijkeboer, M., Guiselin, N., Creach, V., & Artigas, L.F.  
1663 (2015). High-resolution analysis of a North Sea phytoplankton community structure based on in situ flow  
1664 cytometry observations and potential implication for remote sensing. *Biogeosciences*, *12*, 4051-4066

1665 Torrecilla, E., Stramski, D., Reynolds, R.A., Millán-Núñez, E., & Piera, J. (2011). Cluster analysis of  
1666 hyperspectral optical data for discriminating phytoplankton pigment assemblages in the open ocean.  
1667 *Remote Sensing of Environment*, *115*, 2578-2593

1668 Turner, K. J., Mouw, C. B., Hyde, K. J., Morse, R., & Ciochetto, A. B. (2021). Optimization and assessment  
1669 of phytoplankton size class algorithms for ocean color data on the Northeast US continental shelf.  
1670 *Remote Sensing of Environment*, *267*, 112729.

1671 Uitz, J., Claustre, H., Morel, A., & Hooker, S.B. (2006). Vertical distribution of phytoplankton communities  
1672 in open ocean: An assessment based on surface chlorophyll. *Journal of Geophysical Research*, *111*,  
1673 C08005

1674 Uitz, J., Stramski, D., Reynolds, R.A., & Dubranna, J. (2015). Assessing phytoplankton community  
1675 composition from hyperspectral measurements of phytoplankton absorption coefficient and remote-  
1676 sensing reflectance in open-ocean environments. *Remote Sensing of Environment*, *171*, 58-74

1677 van Heukelem, L., & Hooker, S.B. (2011). The importance of a quality assurance plan for method  
1678 validation and minimizing uncertainties in the HPLC analysis of phytoplankton pigments. In C.A.  
1679 Llewellyn, E.S. Egeland, G. Johnsen, & S. Roy (Eds.), *Phytoplankton Pigments: Characterization,*  
1680 *Chemotaxonomy and Applications in Oceanography* (pp. 195-256). Cambridge: Cambridge University  
1681 Press

1682 Vandermeulen, R.A., Mannino, A., Neeley, A., Werdell, J., & Arnone, R. (2017). Determining the optimal  
1683 spectral sampling frequency and uncertainty thresholds for hyperspectral remote sensing of ocean color.  
1684 *Optics Express*, *25*, A785-A797

1685 Vaultot, D., Courties, C., & Partensky, F. (1989). A simple method to preserve oceanic phytoplankton for  
1686 flow cytometric analyses. *Cytometry*, *10*, 629-635

1687 Verbeek, L., Gall, A., Hillebrand, H., & Striebel, M. (2018). Warming and oligotrophication cause shifts in  
1688 freshwater phytoplankton communities. *Global Change Biology*, *24*, 4532-4543

1689 Vidussi, F., Claustre, H., Manca, B.B., Luchetta, A., & Marty, J.-C. (2001). Phytoplankton pigment  
1690 distribution in relation to upper thermocline circulation in the eastern Mediterranean Sea during winter.  
1691 *Journal of Geophysical Research*, *106*, 19939-19956

1692 Vuorio, K., Lepistöe, L., & Holopainen, A.L. (2007). Intercalibrations of freshwater phytoplankton  
1693 analyses. *Boreal Environment Research*, *12*, 561-569

1694 Wang, L., Ou, L., Huang, K., Chai, C., Wang, Z., Wang, X., & Jiang, T. (2018). Determination of the spatial  
1695 and temporal variability of phytoplankton community structure in Daya Bay via HPLC-CHEMTAX pigment  
1696 analysis. *Journal of Oceanology and Limnology*, *36*, 750-760

1697 Wang, S., Xiao, C., Ishizaka, J., Qiu, Z., Sun, D., Xu, Q., Zhu, Y., Huan, Y., & Watanabe, Y. (2016). Statistical  
1698 approach for the retrieval of phytoplankton community structures from in situ fluorescence  
1699 measurements. *Optics Express*, *24*, 23635-23653

1700 Ward, B.A., Dutkiewicz, S., Jahn, O., & Follows, M.J. (2012). A size-structured food-web model for the  
1701 global ocean. *Limnology and Oceanography*, *57*, 1877-1891

1702 Ward, B.A., & Follows, M.J. (2016). Marine mixotrophy increases trophic transfer efficiency, mean  
1703 organism size, and vertical carbon flux. *Proceedings of the National Academy of Sciences*, *113*, 2958-2963

1704 Werdell, P.J., Behrenfeld, M.J., Bontempi, P.S., Boss, E., Cairns, B., Davis, G.T., Franz, B.A., Gliese, U.B.,  
1705 Gorman, E.T., Hasekamp, O., Knobelspiesse, K.D., Mannino, A., Martins, J.V., McClain, C.R., Meister, G., &  
1706 Remer, L.A. (2019). The Plankton, Aerosol, Cloud, Ocean Ecosystem Mission: Status, Science, Advances.  
1707 *Bulletin of the American Meteorological Society*, *100*, 1775-1794

1708 Werdell, P.J., Franz, B.A., Bailey, S.W., Feldman, G.C., Boss, E., Brando, V.E., Dowell, M., Hirata, T.,  
1709 Lavender, S.J., Lee, Z.P., Loisel, H., Maritorena, S., Melin, F., Moore, T.S., Smyth, T.J., Antoine, D., Devred,  
1710 E., d'Andon, O.H.F., & Mangin, A. (2013). Generalized ocean color inversion model for retrieving marine  
1711 inherent optical properties. *Applied Optics*, *52*, 2019-2037

1712 Werdell, P.J., Roesler, C.S., & Goes, J.I. (2014). Discrimination of phytoplankton functional groups using  
1713 an ocean reflectance inversion model. *Applied Optics*, *53*, 4833-4849

1714 Westberry, T., Siegel, D.A., & Subramaniam, A. (2005). An improved bio-optical model for the remote  
1715 sensing of *Trichodesmium* spp. blooms. *Journal of Geophysical Research: Oceans*, *110*

1716 Wilkinson, M.D., Dumontier, M., Aalbersberg, I.J., Appleton, G., Axton, M., Baak, A., Blomberg, N.,  
1717 Boiten, J.-W., ... & Mons, B. (2016). The FAIR Guiding Principles for scientific data management and  
1718 stewardship. *Scientific Data*, *3*, 160018

1719 Willén, E. (1976). A simplified method of phytoplankton counting. *British Phycological Journal*, *11*, 265-  
1720 278

1721 Wolanin, A., Soppa, M.A., & Bracher, A. (2016). Investigation of spectral band requirements for  
1722 improving retrievals of phytoplankton functional types. *Remote Sensing*, *8*, 871

1723 Wolny, J.L., Tomlinson, M.C., Schollaert Uz, S., Egerton, T.A., McKay, J.R., Meredith, A., Reece, K.S., Scott,  
1724 G.P., & Stumpf, R.P. (2020). Current and Future Remote Sensing of Harmful Algal Blooms in the  
1725 Chesapeake Bay to Support the Shellfish Industry. *Frontiers in Marine Science*, *7*

1726 Worden, A.Z., Nolan, J.K., & Palenik, B. (2004). Assessing the dynamics and ecology of marine  
1727 picophytoplankton: The importance of the eukaryotic component. *Limnology and Oceanography*, *49*,  
1728 168-179

1729 Wynne, T.T., R.P. Stumpf, M.C. Tomlinson, R.A. Warner, P.A. Tester, J. Dyble & Fahnenstiel, G.L. (2008).  
1730 Relating spectral shape to cyanobacterial blooms in the Laurentian Great Lakes. *International Journal of*  
1731 *Remote Sensing*, *29*, 3665-3672

1732 Xi, H., Hieronymi, M., Krasemann, H., & Röttgers, R. (2017). Phytoplankton Group Identification Using  
1733 Simulated and In situ Hyperspectral Remote Sensing Reflectance. *Frontiers in Marine Science*, *4*

1734 Xi, H., Hieronymi, M., Röttgers, R., Krasemann, H., & Qiu, Z. (2015). Hyperspectral Differentiation of  
1735 Phytoplankton Taxonomic Groups: A Comparison between Using Remote Sensing Reflectance and  
1736 Absorption Spectra. *Remote Sensing*, *7*, 14781

1737 Xi, H., Losa, S.N., Mangin, A., Garnesson, P., Bretagnon, M., Demaria, J., Soppa, M.A., Hembise Fanton  
1738 d'Andon, O., & Bracher, A. (2021). Global Chlorophyll a Concentrations of Phytoplankton Functional  
1739 Types With Detailed Uncertainty Assessment Using Multisensor Ocean Color and Sea Surface  
1740 Temperature Satellite Products. *Journal of Geophysical Research: Oceans*, *126*, e2020JC017127  
1741 Xi, H., Losa, S.N., Mangin, A., Soppa, M.A., Garnesson, P., Demaria, J., Liu, Y., d'Andon, O.H.F., & Bracher,  
1742 A. (2020). Global retrieval of phytoplankton functional types based on empirical orthogonal functions  
1743 using CMEMS GlobColour merged products and further extension to OLCI data. *Remote Sensing of*  
1744 *Environment*, *240*, 111704  
1745 Xiao, Y., & Friedrichs, M. (2014). The assimilation of satellite-derived data into a one-dimensional lower  
1746 trophic level marine ecosystem model. *Journal of Geophysical Research: Oceans*, *119*, n/a-n/a  
1747 Ye, H., Zhang, B., Liao, X., Li, T., Shen, Q., Zhang, F., Zhu, J., & Li, J. (2019). Gaussian decomposition and  
1748 component pigment spectral analysis of phytoplankton absorption spectra. *Journal of Oceanology and*  
1749 *Limnology*, *37*, 1542-1554  
1750 Yeh, Y.C., McNichol, J., Needham, D.M., Fichot, E.B., Berdjeb, L., & Fuhrman, J.A. (2021). Comprehensive  
1751 single-PCR 16S and 18S rRNA community analysis validated with mock communities, and estimation of  
1752 sequencing bias against 18S. *Environmental Microbiology*, *23*, 3240-3250  
1753 Zapata, M., Jeffrey, S.W., Wright, S.W., Rodríguez, F., Garrido, J.L., & Clementson, L. (2004).  
1754 Photosynthetic pigments in 37 species (65 strains) of Haptophyta: implications for oceanography and  
1755 chemotaxonomy. *Marine Ecology Progress Series*, *270*, 83-102  
1756 Zibordi, G., Voss, K.J., Johnson, B.C., & Mueller, J. (2019). Protocols for Satellite Ocean Colour Sensor  
1757 Validation: In Situ Optical Radiometry. In, IOCCG Protocols Series. Dartmouth, NS, Canada: IOCCG  
1758 Zhang, M., Ibrahim, A., Franz, B.A., Ahmad, Z., & Sayer, A.M. (2022). Estimating pixel-level uncertainty in  
1759 ocean color retrievals from MODIS. *Optics Express*, *30*, 31415-31438  
1760 Zhu, F., Massana, R., Not, F., Marie, D., & Vaultot, D. (2005). Mapping of picoeucaryotes in marine  
1761 ecosystems with quantitative PCR of the 18S rRNA gene. *FEMS Microbiology Ecology*, *52*, 79-92  
1762 Zhu, Q., Shen, F., Shang, P., Pan, Y., & Li, M. (2019). Hyperspectral Remote Sensing of Phytoplankton  
1763 Species Composition Based on Transfer Learning. *Remote Sensing*, *11*, 2001  
1764

1765 Figures and Tables.



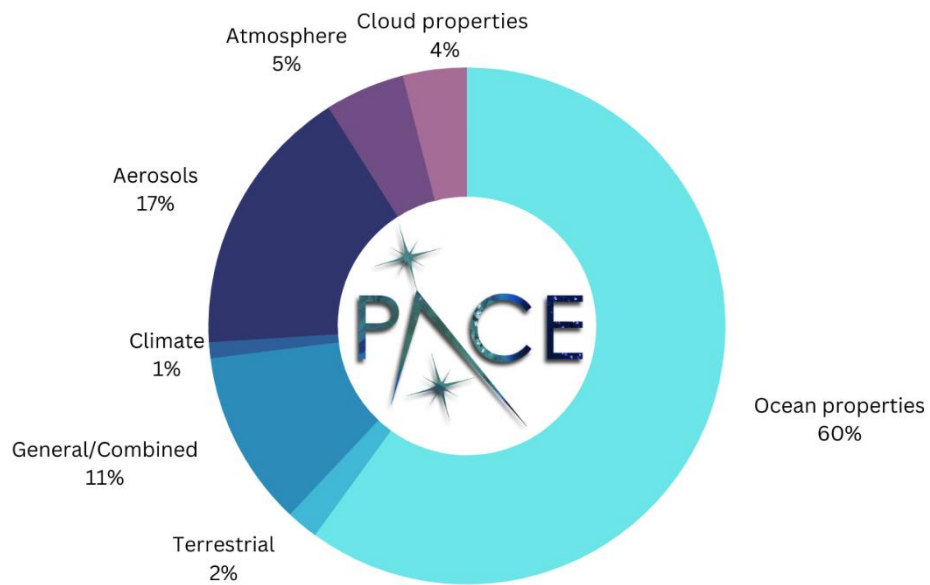
1766

1767 *Figure 1. Artist's rendition of NASA's Plankton, Aerosol, Cloud, ocean Ecosystem satellite flying*  
1768 *over cloud-covered Earth's Ocean. The Ocean Color Instrument is visible on the front of the*  
1769 *platform, while two polarimeters (located on the bottom side of the platform) are not visible from*  
1770 *this view. Credit: NASA Scientific Visualization Studio.*

1771

1772

1773



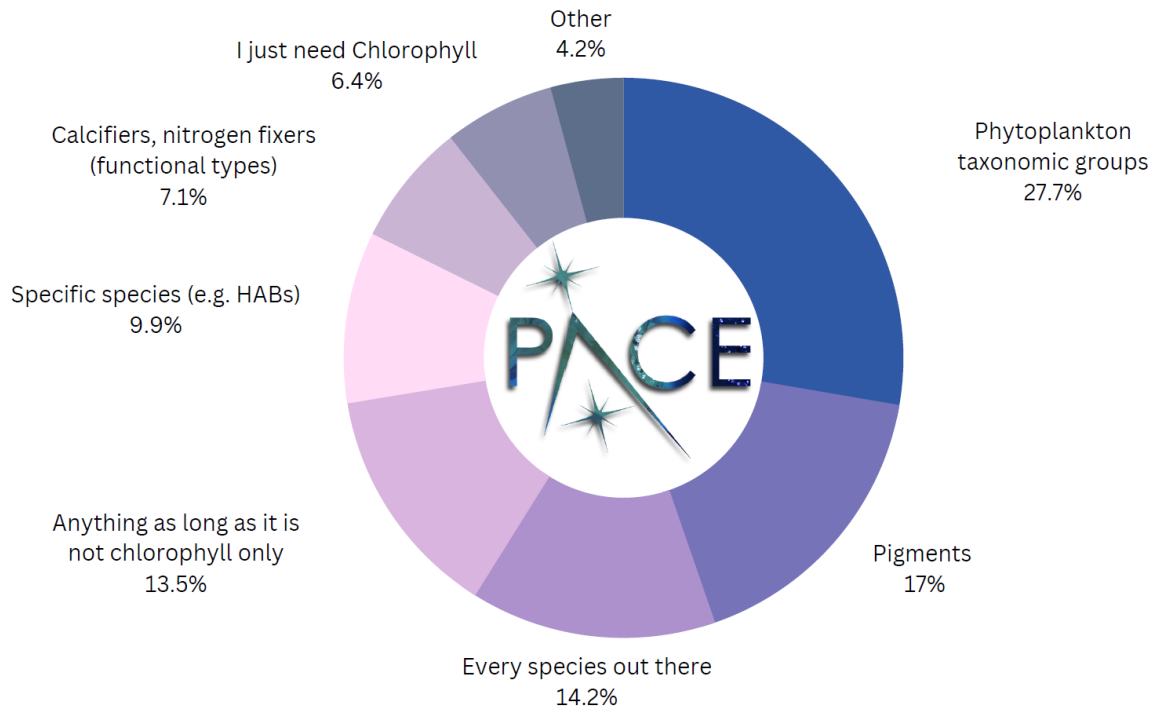
1774

1775 *Figure 2. Self-identified research focus areas grouped into thematic areas, as dictated by PACE*

1776 *Community of Practice members.*

1777

1778

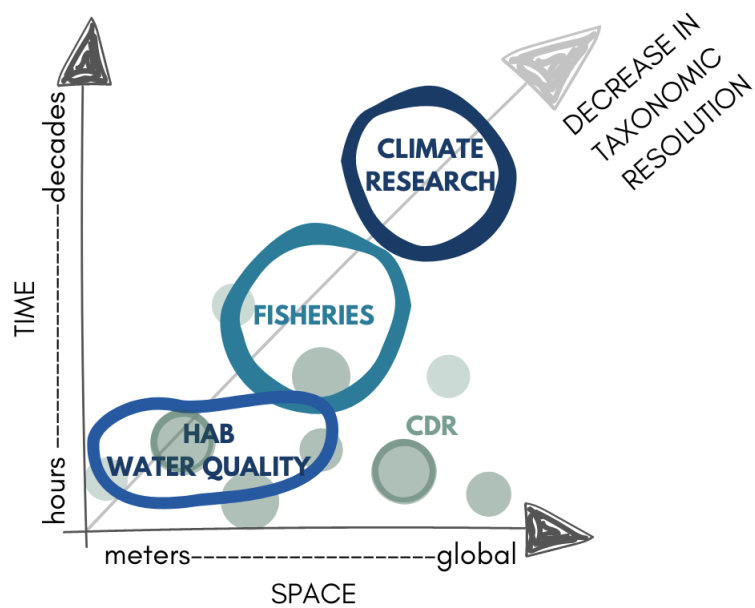


1779

1780 *Figure 3. Needs of the PACE Community of Practice, based on the responses collected from a*

1781 *questionnaire with predetermined answers or other (optionally including a write-in answer).*

1782



1783

1784 Figure 4. PACE will provide data to answer scientific questions about phytoplankton community

1785 composition (PCC) at local to global scales. The user community, already actively engaged in

1786 developing frameworks and pipelines that use PACE data or support mission objectives, comes

1787 from different sectors, whose scientific objectives are sometimes distinct and sometimes

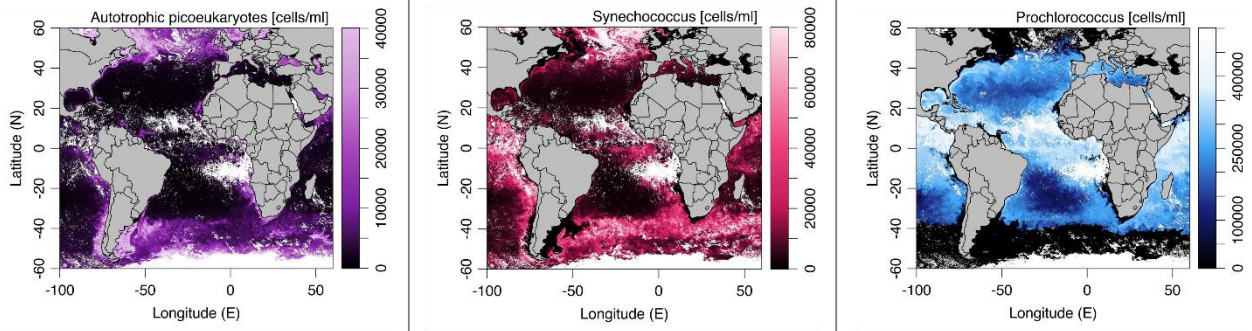
1788 overlapping. This illustration provides example research interests at different scales and from

1789 different sectors.

1790

1791

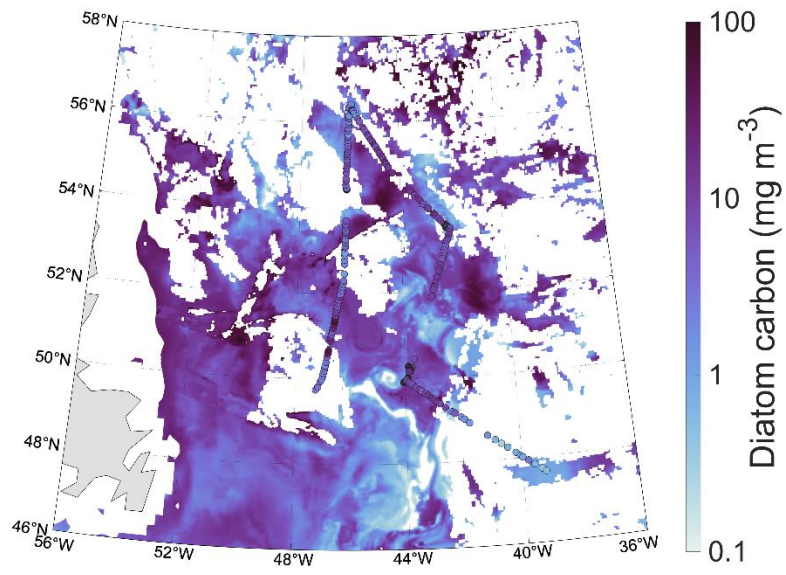
1792



1793

1794 *Figure 5. Spatial distribution of the autotrophic picoeukaryotes, Synechococcus, and Prochlorococcus,*  
1795 *stated as concentration of cells per volume, derived from MODIS Aqua (modified after Lange et al. 2020).*

1796



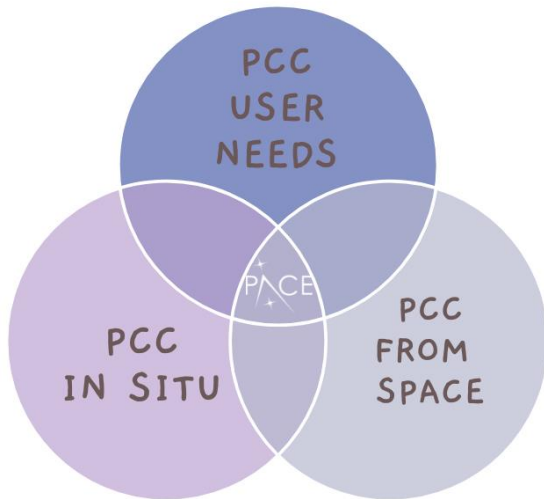
1797

1798 *Figure 6. Diatom Carbon concentration derived from three component neural network model, following*

1799 *Chase et al. 2022.*

1800

1801



1802

1803 *Figure 7. PCC from PACE is an intersection of user's needs, facilitated and constrained by the*  
1804 *spaceborne technology aboard the satellite, and our capability to measure and define the*  
1805 *phytoplankton community structure in-situ.*

1806

1807

1808 *Table 1 Instrument specifications for OCI, HARP2 and SPEXone (modified from Table 2 from*  
 1809 *Werdell et al. (2019))*

	OCI	HARP2	SPEXone
UV-NIR range (bandwidth)	Continuous from 340 to 890nm* in 2.5-nm steps (5)	441 (16), 549 (10), 665 (11), and 866 (40) nm (nominal)	Continuous from 385 to 770 nm in 2-4nm steps
SWIR channels (bandwidth)	940 (45), 1,038 (75), 1,250 (30), 1,378 (15), 1,615 (75), 2,130 (50) and 2,260 (75) nm	None	None
Polarized bands	None	All	Continuous from 385 to 770 nm in 15-45nm steps
Number of viewing angles	One, with fore-aft instrument tilt of $\pm 20^\circ$ to avoid sun glint	10 for 440, 550 and 870 nm and 60 for 670 nm (spaced over $114^\circ$ )	5 ( $-57^\circ, -20^\circ, 0^\circ, 20^\circ, 57^\circ$ )
Swath width	$\pm 56.6^\circ$ (2,663 km at $20^\circ$ tilt)	$\pm 47^\circ$ (1,556km at nadir)	$\pm 4^\circ$ (100 km at nadir)
Global coverage	1-2+ days	2 days	~30 days
Ground pixel	1 km at nadir	3 km	2.5 km
Institution	GSFC	UMBC	SRON/Airbus

1810

1811

1812 Table 2. Comparison of different methods, capabilities, and their connection to expected PACE  
 1813 products (from perspective of algorithm development and validation)

1814

Method	Volume sampled (approx.)	Size range detected (approx.)	Taxonomic resolution	What is actually measured?	PACE-relevant examples
Light microscopy	1-200 mL	10-200 $\mu\text{m}$ (nominal)	To species level	Cell concentrations and/or biovolume (can estimate cellular carbon)	Brewin et al. (2011a); Soto et al. (2015); Wolny et al. (2020)
HPLC pigments	1-10 L	>0.3 $\mu\text{m}$ (nominal; 0.7 $\mu\text{m}$ for non-combusted GF/F)	Group level	Pigment concentrations	Bracher et al. (2015); Chase et al. (2017); Kramer et al. (2022); Uitz et al. (2015)
Flow cytometry	0.1-2 mL	0.2-50 $\mu\text{m}$ (instrument and volume dependent)	<i>Prochlorococcus</i> , <i>Synechococcus</i> , pico- and nano-eukaryotes	Cell concentrations and optical properties (can estimate cellular carbon)	Lange et al. (2020), Kramer et al. (2020)
Imaging-in-flow cytometry	2-5 mL	6-150 $\mu\text{m}$ (nominal)	To species level	Cell concentrations + biovolumes (can estimate cellular carbon)	Chase et al. (2022)
DNA metabarcoding	0.5-10 L	>0.2 $\mu\text{m}$ (filter dependent, nominal)	To species level	Relative sequence abundances and/or barcode gene concentrations	Catlett et al. (2021)

1815

1816

1817

1818

1819 *Table 3. Compilation of published algorithms to assess phytoplankton community composition. Algorithms are considered global if they*  
 1820 *are designed for/applied to more than one major ocean.*

1821

Application	PCC product(s)	Algorithm validation data	Remote sensing approaches	Hyperspectral (or polarization?) in situ approaches	
Global	Taxonomic group(s)	Direct cell observation (cultures and/or field microscopy)	Subramaniam et al. (2001); Westberry et al. (2005) Subramaniam and Carpenter (1994)		
		Pigment concentrations	Alvain et al. (2005); Alvain et al. (2008); Ben Mustapha et al. (2014); Bracher et al. (2009); Hirata et al. (2011); Losa et al. (2017); Moore et al. (2012); Palacz et al. (2013); Sadeghi et al. (2012); Soppa et al. (2014); Xi et al. (2020)	Torrecilla et al. (2011)	
		Spectral signatures	Brown and Yoder (1994)		
	Size classes, size index, or PSD	Pigment concentrations	Brewin et al. (2010); Brewin et al. (2015); Devred et al. (2006); Devred et al. (2011); Fujiwara et al. (2011); Hirata et al. (2008); Hirata et al. (2011); Kostadinov et al. (2010); Li et al. (2013); Moore and Brown (2020); Mouw and Yoder (2010); Roy et al. (2013, spectral_a_ph also used in development); Uitz et al. (2006)		
		Mie modeling, Coated Spheres model	Kostadinov et al. (2009); Kostadinov et al. (2022)		
		Spectral signatures	Bricaud et al. (2012)		
	Accessory pigments	Pigment concentrations	O'Shea et al. (2021); Wang et al. (2018)	Bracher et al. (2015); Chase et al. (2013); (Chase et al. 2017); Kramer et al. (2022); Taylor et al. (2013); Uitz et al. (2015)	
Regional /Local	Taxonomic group(s)	Direct cell observation (microscopy of cultures and/or field data or imaging-in-flow cytometry)	Chase et al. (2022); Raitsos et al. (2008) Réve-Lamarche et al. (2017)	Kirkpatrick et al. (2000); Lubac et al. (2008); Millie et al. (1997); Xi et al. (2017); Xi et al. (2015)	
		Pigment concentrations	Di Cicco et al. (2017); Kramer et al. (2018); Palacios et al. (2015); Sathyendranath et al. (2004); Werdell et al. (2014)	Catlett and Siegel (2018); Isada et al. (2015); Shaju et al. (2015)	
		Spectral signatures		Craig et al. (2006); Wynne et al. (2008)	
	Size classes, size index, or PSD	Pigment concentrations	Gittings et al. (2019)		
		Spectral signatures	Ciotti and Bricaud (2006)		
	Accessory pigments	Pigment concentrations	Bracher et al. (2015); Pan et al. (2010); Sun et al. (2022)	Aguirre-Gómez et al. (2001); Hoepffner and Sathyendranath (1991); Hoepffner and Sathyendranath (1993); Liu et al. (2019); Lohrenz et al. (2003); Wang et al. (2016); Ye et al. (2019)	

1822

1823

1824 *Table 4. Acronyms and symbols used in the text.*

CDOM	Colored Dissolved Organic Matter
CDR	Carbon Dioxide Removal
CHEMTAX	CHEMical TAXonomy
CHIME3	Copernicus Hyperspectral Imaging Mission for the Environment
<i>Chl a</i>	Chlorophyll a
CMIP	Climate Research Programme Coupled Model Intercomparison Project
CoP	Community of Practice
DNA	Deoxyribonucleic Acid
EOSDIS	NASA's Earth Observing System Data and Information System
EOV	Essential Ocean Variable
ESM	Earth System Models
FAIR	Findable, Accessible, Interoperable and Reusable
FCM	Flow cytometry
GIOP	Generalized IOP algorithm
GLIMR	Geosynchronous Littoral Imaging and Monitoring Radiometer
GSFC	Goddard Space Flight Center
HABs	Harmful Algal Blooms
HARP2	Hyper Angular Research Polarimeter
HICO	Hyperspectral Imager for the Coastal Ocean
HNLC	High Nutrient Low Chlorophyll
HPLC	High performance liquid chromatography
IFCB	Imaging FlowCytobot
IOCCG	<i>International Ocean-Colour Coordinating Group</i>
IPCC	Intergovernmental Panel on Climate Change
GCOM-C	Global Change Observation Mission – Climate satellite
JAXA	Japan Aerospace Exploration Agency
LEO	Low Earth Orbit
MAAs	Mycosporine-like Amino Acids
MERIS	Medium Resolution Imaging Spectrometer
MODIS	Moderate Resolution Imaging Spectroradiometer
NASA	National Aeronautics and Space Administration
NASA NOMAD	NASA bio-Optical Marine Algorithm Dataset
NIR	Near-Infrared
OB.DAAC	NASA's Ocean Biology Distributed Active Archive Center
OCI	Ocean Color Instrument
PACE	NASA's Plankton, Aerosol, Cloud, ocean Ecology
PAR	Photosynthetically Active Radiation
PCC	Phytoplankton Community Composition
PhytoDOAS	Extension of the Differential Optical Absorption Spectroscopy (DOAS, a method for detection of atmospheric trace gases), developed for remote identification of oceanic phytoplankton groups
POLDER	Polarization and Directionality of the Earth's Reflectance
PSC	Phytoplankton Size Class
$R_{rs}(\lambda)$	Remote Sensing Reflectance

SBG	Surface Biology and Geology mission
SCIAMACHY	Scanning Imaging Absorption Spectrometer for Atmospheric Chartography
SeaBASS	SeaWiFS Bio-optical Archive and Storage System
SeaWiFS	Sea-viewing Wide Field-of-view Sensor
SMD	Science Mission Directorate
SPEXone	Spectro-polarimeter for Planetary Exploration
SPM	Suspended Particulate Matter
SRON	Netherlands Institute for Space Research
SST	Sea Surface Temperature
SWIR	Short-wave Infrared
TOA	Top-of-atmosphere
UMBC	University of Maryland, Baltimore County
UV	Ultraviolet
UVP	Underwater Vision Profiler
VIIRS	Visible Infrared Imaging Radiometer Suite

1825